# Asset Diversification versus Climate Action

Christoph Hambel[a] Holger Kraft[b] Frederick van der Ploeg[c]

Current version: May 22, 2020

**Abstract:** Asset pricing and climate policy are analyzed in a global economy where consumption goods are produced by both a green and a carbon-intensive sector. We allow for endogenous growth and three types of damages from global warming. It is shown that, initially, the desire to diversify assets complements the attempt to mitigate economic damages from climate change. In the longer run, however, a trade-off between diversification and climate action emerges. We derive the optimal carbon price, the equilibrium risk-free rate, and risk premia. Climate disasters, which are more likely to occur sooner as temperature rises, significantly affect asset prices.

**Keywords:** climate finance, decarbonization, diversification, carbon price, asset prices, green assets, disaster risk

**JEL subject codes**: D81, G01, G12, Q5, Q54

[a] Faculty of Economics and Business Administration, Goethe University, Theodor-W.-Adorno-Platz 3, 60323 Frankfurt am Main, Germany. Phone: +49 (0) 69 798 33687.
E-mail: christoph.hambel@finance.uni-frankfurt.de

[b] Faculty of Economics and Business Administration, Goethe University, Theodor-W.-Adorno-Platz 3, 60323 Frankfurt am Main, Germany. Phone: +49 (0) 69 798 33699.
E-mail: holgerkraft@finance.uni-frankfurt.de

[c] University of Oxford, Department of Economics, OXCARRE, Manor Road Building, Oxford OX1 3UQ, U.K. Phone: +44 (0) 1865 281285.
E-mail: rick.vanderploeg@economics.ox.ac.uk. Also affiliated with Free University of Amsterdam, The Netherlands.

We thank Patrick Bolton, Stavros Panageas, Armon Rezai, Eduardo Schwartz, Frank Venmans, and the participants of the EBI Global Annual Conference 2020 for helpful comments and suggestions. All remaining errors are our own. Christoph Hambel and Holger Kraft gratefully acknowledge financial support by Deutsche Forschungsgemeinschaft (DFG).

# Asset Diversification versus Climate Action

Current version: May 22, 2020

**Abstract:** Asset pricing and climate policy are analyzed in a global economy where consumption goods are produced by both a green and a carbon-intensive sector. We allow for endogenous growth and three types of damages from global warming. It is shown that, initially, the desire to diversify assets complements the attempt to mitigate economic damages from climate change. In the longer run, however, a trade-off between diversification and climate action emerges. We derive the optimal carbon price, the equilibrium risk-free rate, and risk premia. Climate disasters, which are more likely to occur sooner as temperature rises, significantly affect asset prices.

**Keywords:** climate finance, decarbonization, diversification, carbon price, asset prices, green assets, disaster risk

**JEL subject codes**: D81, G01, G12, Q5, Q54

# 1 Introduction

Climate change impacts all areas of human life and impacts economic activity.[1] To avoid carbon-dioxide emissions, emissions-free technologies and renewable energies are developed. Depending on the perceived severity of the consequences of climate change, there are different opinions about how urgent it is to transition to a less carbon-intensive economy. We are interested in the interplay between financial considerations and policies to mitigate climate change and answer two key questions. First, does the financial need to diversify assets hamper or help the fight against climate policy and how does it affect the optimal carbon price? Second, how does climate change and the desire to combat it affects the pricing of green and dirty assets? We show that there is a subtle dynamic interdependence between the financial goal to diversify assets in portfolios and the environmental goal to reduce carbon emissions.

Our economic framework is a stochastic macroeconomic growth model with two capital stocks and two energy sources. The green sector takes carbon-free energy as input (green energy). The dirty sector is carbon-intensive and requires fossil fuel whose combustion leads to carbon emissions. There are two types of capital stocks. Investments and capital reallocation from the dirty to the green capital stock are both subject to adjustment costs. Capital stock accumulation is exposed to diffusive shocks as well as the risk of macroeconomic disasters. Emissions are proportional to fossil fuel use.

Exploiting recent advances in climate science, we assume that global temperature is proportional to cumulative emissions.[2] We allow for three potential channels for the effect of climate change on economic activity. First, higher temperature leads to a higher share of damages in pre-damage output as in the seminal DICE-2016R2 model; see, e.g. Nordhaus (2017). Second, higher temperatures might negatively affect the growth rate of capital; e.g., Dell et al. (2009, 2012). Third, higher temperatures may increase the Poisson risk of a climate-related disaster; e.g. Bansal et al. (2019) or Karydas and Xepapadeas (2019).

We first establish a crucial dynamic relation between the intensity of climate action as measured by the size of the optimal carbon price and the economic motive to diversify. Initially, the dirty capital stock dominates the economy and there are two complementary goals: the first one is to mitigate climate change and thus to decarbonize the economy; the second goal is to diversify the

[1] See, e.g., Scheffers et al. (2019).

[2] See Matthews et al. (2009), Allen et al. (2009), IPCC (2014), van der Ploeg (2018), and Dietz and Venmans (2019), among others, for further references.

economy, which is a purely financial goal. Both goals incentivize the agent to actively reduce the dirty capital stock. The speed of the transition towards a zero-emissions economy is thus amplified by the diversification motive. Over time, however, the two goals start to conflict and a trade-off arises. From a diversification perspective, the process should be stopped if there is a balance between green and dirty capital.[3] From an environmental perspective the dirty capital stock should eventually be run down completely. Our various calibrations show, however, that this does not occur unless climate change is perceived as extremely severe (relative to the global warming damages allowed for in well-established models such as the DICE model (Dynamic Integrated Model of Climate and the Economy) of Nordhaus (2017)). Effectively, diversification considerations prevent the agent from driving the carbon-intensive capital stock to zero.

Second, we investigate the interplay between climate change and the pricing of green and dirty assets. We analyze the dynamics of the risk-free rate and risk premia during the transition from a carbon-intensive towards a zero-emissions economy. To separate economic from climate effects, our model involves the risk of macroeconomic disaster shocks as in Barro (2006, 2009) and Pindyck and Wang (2013). Therefore, our model can generate a high equity premium and a low risk-free rate as observed in historical data when climate change has had no significant impact on the economy. Taking the effects of climate change into account, our findings for the risk-free rate and risk premia in an economy affected by climate change are different: regardless of how climate change affects the economy, the risk-free interest rate decreases in response to rising temperatures. By contrast, risk premia are only significantly affected if we allow for potential climate disasters for which the probability of them occurring increases with temperature. Without such disasters, the impact on risk premia is moderate.

We enrich a well-known asset pricing framework by adding the climate module of an integrated assessment model (IAM). It is thus related to several strands of the literature: the asset-pricing component involves a model of macroeconomic disasters that has been developed by Barro (2006, 2009) and Wachter (2013), among others. Besides, our representative agent has recursive utility as in Bansal and Yaron (2004) or Pindyck and Wang (2013). We consider a production economy with two sectors. Therefore, capital is endogenous and the agent has control over the size of the sectors. If the size of the sectors were exogenous and the effect of climate change is disregarded, then the two-tree model analyzed in Cochrane et al. (2007) arises as special case.

[3] If both capital stocks are equally volatile, this balance is reached when they are of equal size.

The climate component is related to the literature on integrated assessment models of the economy and the climate. These studies typically have one sector and do not focus on asset pricing. For example, the celebrated DICE model is a widely used framework to study optimal carbon abatement and carbon pricing. It combines a Ramsey-type model for capital allocation with deterministic dynamics of emissions, carbon dioxide and global temperature. The original model is formulated in a deterministic setting, see for example Nordhaus (1992) and Nordhaus (2017). In frameworks with recursive utility, Crost and Traeger (2014), Jensen and Traeger (2014), Ackerman et al. (2013), Bretschger and Vinogradova (2019), van den Bremer and van der Ploeg (2019) analyze versions with stochastic elements. Cai and Lontzek (2019) study a stochastic generalization of the DICE model involving stochastic growth and the risk of tipping points. Furthermore, there are IAM frameworks that do not fall into the class of DICE models. For instance, Golosov et al. (2014) obtain closed-form solutions in a framework with log utility, Cobb-Douglas production and full depreciation in one discrete time period, and damages that are an exponential function of the atmospheric carbon stock. Traeger (2019) generalizes this setting to recursive preferences and provides a description of the carbon cycle and the climate system and also allows for epistemological uncertainty and anticipated learning.

There are few papers that combine an asset pricing framework with an integrated assessment model. An important paper that explores the implications of asset pricing for climate policy is Barnett et al. (2020), who analyze a stochastic one-sector macroeconomic DSGE model of endogenous growth with stochastic economic growth rates and endogenous investments in fossil fuel reserves. They also address the issue of preference-based concerns about ambiguity and model misspecification. Using exogenous climate dynamics, Bansal et al. (2017, 2019) quantify the impact of local temperature on asset prices. They study a global long-run risk model that simultaneously matches the observed temperature and consumption growth dynamics. Furthermore, their model is able to generate a low risk-free interest rate and a high equity premium. Similar results are obtained by Donadelli et al. (2017). Karydas and Xepapadeas (2019) study an economy with two assets, but focus on a Lucas-tree endowment economy where the agent cannot actively control the transition to a low-carbon economy. By contrast, van den Bremer and van der Ploeg (2019) study a one-sector production economy with endogenous climate change and a wide range of economic and climatic uncertainties that generates low risk-adjusted interest rates and a high risk premium. Furthermore, Dietz et al. (2018) address the question of whether fighting climate change could be a hedge against macroeconomic risk.

Finally, Daniel et al. (2019) show in a stylized setting that recursive preferences with general resolution of uncertainty about climate change can lead to a declining carbon price.[4]

The remainder of the paper is structured as follows: Section 2 introduces the model setup. Section 3 explains our approach to solving for the social optimum and discusses how the social optimum can be decentralized in the market economy. Section 4 discusses our calibration strategy. Section 5 presents our main results on the relation between the diversification motive and climate action. Section 6 discusses how climate change affects the equilibrium risk-free rate and the risk premia in the economy. Section 7 reports simulation results for our three types of specifications for global damages. Section 8 concludes. The Appendices provides additional material such as proofs and calibration details.

# 2 Model Setup

We present a dynamic two-sector production economy with endogenous growth and production damages resulting from global warming. The green sector uses a carbon-free energy form as input, whereas the carbon-emitting sector also referred to as the dirty sector deploys fossil fuel leading to carbon emissions, global warming and damages to aggregate output. Temperature is driven by cumulative carbon emissions. A representative agent decides how to allocate resources to both trees. Energy inputs are unconstrained available.This agent can also reallocate capital from the dirty capital stock to the green capital stock. Both investment and reallocation are costly. The agent has recursive preferences with unit elasticity of intertemporal substitution and a certain coefficient of relative risk aversion. In the following, we describe the model components in detail.

## 2.1 Production of Goods

Final goods can be produced in two sectors. The outputs of these two sectors are perfect substitutes. The first sector is the carbon-free or green sector and the second sector is the dirty sector. We suppose that the capital stock used in each sector is a broad measure which also boosts the productivity of labor. We assume that the outputs of both sectors are given by the Cobb-Douglas production functions $Y_n = A_n K_n^{\alpha_n} F_n^{\eta_n} (K_n L_n)^{1-\alpha_n-\eta_n} \Lambda_i(T)$, $n \in \{1, 2\}$,

[4]The feature of a declining carbon price is derived from a binomial tree with a fixed horizon.

where $K_n$ is the capital stock of sector $n$ and $L_n$ is labor supply which is a fixed factor set to unity without loss of generality. The rate of energy use in sector $n$ is denoted by $F_n$ where we refer to $F_1$ as *green energy* and to $F_2$ as *fossil fuel use* which causes carbon dioxide emissions. The Cobb-Douglas weights $\alpha_n$ and $\eta_n$ as well as total factor productivity $A_n$ are non-negative, sector-specific constants, and $\alpha_n + \eta_n < 1$. Here, $T$ denotes the global average temperature increase measured relative to the beginning of the industrial revolution. Therefore, $T = 0$ is the pre-industrial level of temperature and $T = 2$ is a temperature of two degrees above the pre-industrial level.

The function $\Lambda_n$ is a sector-specific function that shows how much output is curbed in response to higher temperatures; see, e.g., Nordhaus and Sztorc (2013). This is the *first channel* by which climate change influences economic activity. In the sequel, we introduce two other channels by which temperature curbs economic activity.[5]

In line with endogenous growth theory, at the aggregate level we have constant returns to scale with respect to capital and energy, i.e.,

$$Y_n = A_n K_n^{1-\eta_n} F_n^{\eta_n} \Lambda_n(T) \tag{2.1}$$

is the output of sector $n$. In contrast to the long-run exogenous growth rates stemming from labor-augmenting technical progress and population growth in classical growth theory, we have endogenous technical progress captured by the broad measure of capital boosting the efficiency of labor and thus ensuring that production at the aggregate level has constant returns to scale with respect to capital and energy. Since the two final goods are perfect substitutes in consumption, aggregate output is $Y = Y_1 + Y_2$. We could have adopted a more realistic production structure with imperfect substitution between the two final goods and with each final goods sector having both types of energy and capital stocks as production factor. Also, one could argue that once the energy transition from coal to solar energy has taken place, electricity is a uniform good, see Hassler et al. (2020). However, we have chosen this simple structure to highlight our key mechanisms.

[5]These are a growth-rate effect and a temperature dependence of the disaster intensity $\lambda$, see (2.2) and (2.3) below.

## 2.2 Investments in Green and Dirty Capital

Let $I_n$ be the investment rate in sector $n$ and $R$ the rate at which carbon-emitting capital can be converted into green capital. Investment is subject to quadratic intertemporal adjustment costs. The conversion of dirty into green capital generates quadratic intrasectoral adjustment costs. Intuitively, one dollar of dirty capital can be converted into less than one dollar of green capital where the wedge increases in the amount being converted. The depreciation rates of the physical capital stocks in the absence of global warming are denoted by $\delta_n^k \geq 0$, $n \in \{1, 2\}$.

We allow for an additional component which potentially increases in temperature $T$. The constants $\xi_1$ and $\xi_2$ capture the adverse effects of global warming on the depreciation and growth rates of capital. This effect is suggested by the empirical findings of Dell et al. (2009, 2012) who find a negative impact of global warming on the economic growth rate of developing countries. This is the *second channel* by which climate change can effect economic activity. The capital stock dynamics of the green and dirty sector are then given by[6]

$$\begin{aligned} \mathrm{d}K_1 = &\Big(I_1 - \frac{1}{2}\phi_1 \frac{I_1^2}{K_1} + R - \frac{1}{2}\kappa \frac{R^2}{K_1} - (\delta_1^k + \xi_1 T)K_1\Big)\mathrm{d}t + K_1\sigma_1 \mathrm{d}W_1 \\ &- K_{1-}\Big(\ell_e \mathrm{d}N_e + \ell_c \mathrm{d}N_c\Big), \end{aligned} \tag{2.2}$$

$$\begin{aligned} \mathrm{d}K_2 = &\Big(I_2 - \frac{1}{2}\phi_2 \frac{I_2^2}{K_2} - R - (\delta_2^k + \xi_2 T)K_2\Big)\mathrm{d}t + K_2\sigma_2\Big(\rho_{12}\mathrm{d}W_1 + \sqrt{1-\rho_{12}^2}\mathrm{d}W_2\Big) \\ &- K_{2-}\Big(\ell_e \mathrm{d}N_e + \ell_c \mathrm{d}N_c\Big), \end{aligned} \tag{2.3}$$

where the constants $\phi_n$, $n = 1, 2$, are the investment adjustment cost parameters, $\kappa$ is the capital reallocation cost parameter,[7] and $W_1$ and $W_2$ are two independent Brownian motions. The parameter $\rho_{12}$ denotes the instantaneous correlation coefficient between the Brownian shocks of the two capital stocks. Besides, $N_e$ and $N_c$ are two independent point process capturing disaster risk.

The process $N_e$ models macroeconomic disasters whose jump intensity $\lambda_e$ is constant as in Barro (2006, 2009) and Barro and Jin (2011). The process $N_c$ models climate disasters as in Karydas and Xepapadeas (2019). This is the *third channel* by which climate change can affect

[6] For notational convenience, we drop the time index $t$ whenever it does not create confusion. Furthermore, $K_{n-}$ is short for $K_{nt-}$, i.e., for the left-limit of $K_n$ at time $t$. Notice that for the $\mathrm{d}t$ and $\mathrm{d}W$ terms this distinction is irrelevant since the point process $N$ only jumps at countably many time points and Lebesgue and Brownian integrands can be changed at countably many points.

[7] We assume that the green sector incurs the capital reallocation costs.

the economy. Its jump intensity $\lambda_c = \lambda_c(T)$ depends on current temperature $T$. Intuitively, $\lambda_i \mathrm{d}t$ is the probability for a jump to occur over the small time interval $\mathrm{d}t$ and $1/\lambda_i$ is the expected waiting time to the next jump, $i \in \{e, c\}$. The parameters $\ell_e$ and $\ell_c$ are the corresponding jump sizes which are stochastic, but independent of the Brownian and Poisson shocks in the model. For simplicity, we capture the relative impact of disaster risk by $\ell_i$, which is the same for both types of capital.

To summarize, our model involves *three potential channels* by which climate damages affect the economy. First, there can be a level damage via the damage functions $D_i(T)$ scaling down output in response to climate change. This is the channel that is used in the DICE model. Second, higher temperatures can negatively affect the growth rate of capital and thus output and consumption via the damage parameters $\xi_i$ as in Dell et al. (2009, 2012). Third, the disaster probability might increase in temperature as, for instance, in Bansal et al. (2019) or Karydas and Xepapadeas (2019).

## 2.3 Emissions and Temperature

Following Allen et al. (2009), Matthews et al. (2009), and IPCC (2014), among others, we assume that—up to some environmental stochastic shocks—global average temperature $T$ is driven by cumulative emissions $E_t = \int_0^t \varepsilon_s \mathrm{d}s$ measured in gigatons of carbon (GtCs). Global average temperature (above the pre-industrial level) is thus given by

$$T_t = T_0 + \vartheta E_t + \int_0^t \sigma_T \mathrm{d}W_{3s},$$

where $T_0$ is the current temperature and $\vartheta$ denotes the transient climate response to cumulative emissions (TCRE). Besides, $W_3$ denotes a third standard Wiener process that is independent of $W_1$ and $W_2$. The diffusion coefficient $\sigma_T$ is constant. Current emissions are given by $\varepsilon = \nu F_2$ where $F_2$ denotes the rate of fossil use in energy units and $\nu = \nu(t, T, K_1, K_2)$ is the emission intensity per unit of fossil fuel, which might be state dependent. Consequently, we obtain the following stochastic temperature dynamics

$$\mathrm{d}T = \beta F_2 \mathrm{d}t + \sigma_T \mathrm{d}W_3, \tag{2.4}$$

where $\beta = \vartheta\nu$ and thus $\beta$ might depend on $t$, $T$, $K_1$, and $K_2$. We calibrate the emission intensity such that business-as-usual (BAU) emissions are close to the uncontrolled path in the latest version of DICE, see Nordhaus (2017).[8] Additionally, $\varepsilon = 0$ if $K_2 = 0$, i.e., there are no carbon emissions if the dirty capital stock has been fully phased out.

## 2.4 Dividends, Consumption, and Preferences

The dividend of a sector is defined as the sector's residual cash flow net of investments and energy costs, $D_n = Y_n - I_n - b_n F_n$, where $b_1$ denotes the cost of one unit of renewable energy and $b_2$ the cost of one unit of fossil fuel.[9] For simplicity, we make the bold assumption that the costs of one unit of fossil fuel or renewable energy are exogenous and not affected by exogenous rates of technical progress (e.g., ongoing hikes in green innovation or the shale gas revolution). In equilibrium, aggregated dividends must equal aggregate consumption, i.e., $C = D_1 + D_2$. Our economy is populated by identical agents with recursive preferences. As shown in Duffie and Epstein (1992b),[10] these preferences are the continuous-time version of discrete-time recursive utility developed in Kreps and Porteus (1978) and Epstein and Zin (1989). As in Wachter (2013), among others, we consider the case of unit elasticity of intertemporal substitution (EIS = 1). The coefficient $\gamma$ of relative risk aversion (RRA) can be chosen independently and typically exceeds unit EIS to reflect a preference for early resolution of uncertainty.

The indirect utility function (or value function) $J$ is thus recursively defined by

$$J(t, K_1, K_2, T) = \sup_{I_1, I_2, R, F_1, F_2} \mathbb{E}_t\Big[\int_t^\infty f(C_s, J(s, K_{1s}, K_{2s}, T_s)\mathrm{d}s\Big], \tag{2.5}$$

where $f$ is the aggregator determining preferences. For unit EIS and an arbitrary level of risk aversion $\gamma$, this aggregator takes the form

$$f(C, J) = \begin{cases} \delta(1-\gamma)J \log\Big(\frac{C}{[(1-\gamma)J]^{\frac{1}{1-\gamma}}}\Big), & \gamma \neq 1, \\ \delta\big[\log(C) - J\big], & \gamma = 1, \end{cases}$$

[8] We define the BAU scenario for the decentralized market economy as one where policy makers do not impose carbon taxes.

[9] Some authors define dividends as levered consumption $D_n = C_n^\varphi$ for a leverage parameter $\varphi > 1$ to model a higher volatility of dividends compared to consumption, e.g., Bansal and Yaron (2004), Benzoni et al. (2011), Wachter (2013), Branger et al. (2016).

[10] They refer to this class of preferences as stochastic differential utility (SDU).

where $C$ denotes consumption and $\delta$ the rate of time impatience. Notice that $f$ depends on the indirect utility function $J$, which reflects the recursive structure of the preferences. For $\gamma = 1$, the preference structure collapses to time-additive logarithmic utility.

# 3 Optimality and the Social Cost of Carbon

The indirect utility function $J = J(t, K_1, K_2, T)$ satisfies the Hamilton-Jacobi-Bellman (HJB) equation. Following Duffie and Epstein (1992b), this equation is

$$\begin{aligned} 0 = \max_{I_1, I_2, R, F_1, F_2} \Bigg\{ & J_t + \delta(1-\gamma) J \log\Big(\frac{Y_1 + Y_2 - I_1 - I_2 - b_1 F_1 - b_2 F_2}{[(1-\gamma)J]^{\frac{1}{1-\gamma}}}\Big) + J_T \beta F_2 \\ & + \frac{1}{2} J_{TT} \sigma_T^2 + J_{K_1}\Big(I_1 - \frac{1}{2}\phi_1 \frac{I_1^2}{K_1} + R - \frac{1}{2}\kappa \frac{R^2}{K_1} - (\delta_1^k + \xi_1 T) K_1\Big) + \frac{1}{2} J_{K_1 K_1} K_1^2 \sigma_1^2 \\ & + J_{K_2}\Big(I_2 - \frac{1}{2}\phi_2 \frac{I_2^2}{K_2} - R - (\delta_2^k + \xi_1 T) K_2\Big) + \frac{1}{2} J_{K_2 K_2} K_2^2 \sigma_2^2 + J_{K_1 K_2} K_1 K_2 \sigma_1 \sigma_2 \rho_{12} \\ & + \lambda_e \mathbb{E}[J(K_1(1-\ell_e), K_2(1-\ell_e), T) - J] + \lambda_c(T) \mathbb{E}[J(K_1(1-\ell_c), K_2(1-\ell_c), T) - J] \Bigg\} \end{aligned} \tag{3.1}$$

where subscripts of $J$ denote partial derivatives, e.g., $J_{K_1} = \frac{\partial J}{\partial K_1}$. The first-order optimally conditions give rise to five efficiency conditions.

## 3.1 Optimal Policies

The optimal investment rate in sector $n \in \{1, 2\}$ reads

$$I_n = \frac{K_n}{\phi_n} \frac{q_n - 1}{q_n}, \tag{3.2}$$

where $\phi_n$ is a constant capturing the strength of the adjustment costs and

$$q_n = \frac{C}{\delta(1-\gamma)} \frac{J_{K_n}}{J}, \tag{3.3}$$

is Tobin's Q of sector $n$ to be determined in equilibrium. The optimal reallocation from dirty to green capital is

$$R = \frac{K_1}{\kappa} \frac{q_1 - q_2}{q_1}. \tag{3.4}$$

The optimal use of green energy and fossil fuel follow from

$$\eta_1 A_1 \Big(\frac{F_1}{K_1}\Big)^{\eta_1 - 1} = b_1, \qquad \eta_2 A_2 \Big(\frac{F_2}{K_2}\Big)^{\eta_2 - 1} = b_2 + \tau_f, \tag{3.5}$$

where $\tau_f$ denotes the optimal Pigouvian social cost for using one unit of fossil fuel

$$\tau_f = \frac{\beta C}{\delta(\gamma - 1)} \frac{J_T}{J}. \tag{3.6}$$

The optimal social cost of burning one ton of carbon or SCC for short is thus

$$\tau_c = \frac{\tau_f}{\nu} = \frac{\vartheta C}{\delta(\gamma - 1)} \frac{J_T}{J}, \tag{3.7}$$

where $\nu$ is the emission intensity per unit of fossil fuel defined in Section 2.3. The optimal SCC increases in consumption reflecting that higher economic activity leads to higher carbon taxes; see, e.g., Nordhaus (1991), Golosov et al. (2014), and Rezai and van der Ploeg (2016).

Condition (3.2) for investment in sector $n$ shows that investment rates are small if intertemporal adjustment costs are high and the sectoral Tobin's Q is high. The sectoral Tobin's Q (3.3) is defined as the marginal value of capital converted into utility units. It equals the ratio of market value to the replacement cost of physical value. The sectoral Tobin's Q is bigger than one, since installing capital is costly and installed capital earns a rent in equilibrium.

Condition (3.4) for reallocation determines the rate at which carbon-intensive capital is optimally converted into carbon-free capital. It is proportional to the carbon-free capital stock. Reallocation decreases in the Tobin's Q of the dirty sector and increases in the Tobin's Q of the green sector. This conversion rate is lower if intratemporal adjustment costs are higher.

The two conditions in (3.5) characterize energy use. The marginal product of the green capital stock is equal to the marginal cost of one unit of green energy. For the dirty capital stock, the marginal revenue equals the marginal costs plus the external effects of emitting carbon as measured by the SCC.

The share of dirty capital to total capital is

$$S = \frac{K_2}{K_1 + K_2} \tag{3.8}$$

which indicates the carbon-intensity of the economy. We denote the total stock of capital by $K = K_1 + K_2$. During the transition to a low-carbon economy, carbon-free capital is gradually replacing dirty capital so that the share of dirty capital $S$ decreases over time.

## 3.2 Reduced-Form Indirect Utility Function

To solve the Hamilton-Jacobi-Bellman equation (3.1), we first reduce the number of state variables by one. We define $i_n = I_n/K_n$, $f_n = F_n/K_n$, and $r = R/K_1$. We express the indirect utility function as a function of time and the state variables total capital $K$, share of dirty capital $S$, and temperature $T$ (instead of $K_1$, $K_2$, and $T$). Appendix A shows that the indirect utility function satisfies the following separation.

**Proposition 3.1** (Representation of Indirect Utility)**.** *The solution to the HJB equation (3.1) is of the following form*

$$J(t, K_1, K_2, T) = \frac{1}{1-\gamma}(K_1 + K_2)^{1-\gamma} G\big(t, T, S(K_1, K_2)\big) = \frac{1}{1-\gamma} K^{1-\gamma} G(t, T, S), \tag{3.9}$$

*where the reduced-form indirect utility function $G$ satisfies a modified HJB equation given by equation (A.8) in Appendix A.*

We solve the modified HJB equation with a finite-differences approach. Since the function $G$ depends on two instead of three state variables, this is computationally less demanding. Technical details are given in Appendix C.1. Using the representation (A.1), we obtain a simplified representation of expression (3.7) for the optimal SCC.

**Corollary 3.2** (Social Cost of Carbon)**.** *The optimal social cost of carbon equals*

$$\tau_c = \frac{\vartheta C}{\delta(\gamma - 1)} \frac{G_T}{G},$$

*where the reduced indirect utility function $G$ satisfies the modified HJB equation (A.8). Optimal consumption $C$ is given by equation (A.7).*

## 3.3 Decentralizing the Social Optimum in the Market Economy

There are various ways of ensuring that the social optimum is attained in the decentralized market economy. The most obvious one is to price carbon (either via a global carbon tax or

via a global cap-and-trade system) at a price equal to the optimal SCC and to subsidize capital in sector $n$ at a rate equal to $(1-\eta_n-\alpha_n)Y_n/K_n$. The net revenue of the carbon tax and the capital subsidies to the two sectors is refunded in lump-sum fashion to the private sector. If this is done, it is straightforward to demonstrate that the first-order optimality conditions for the market economy coincide with those of the social optimum. The carbon tax is needed to internalize the global warming externality and the capital subsidies are needed to correct for the fact that firms do not internalize the beneficial effect of capital accumulation (including knowledge creation) on the productivity of labor in other firms.

# 4 Calibration

[Table 1 about here.]

This section discusses the benchmark calibration of our model. Table 1 summarizes the calibration details. Further details can be found in Appendix D.

## 4.1 Economic Growth

In the past, the influence of climate change on asset markets has been negligible and, in general, the historical impact of climate change on the economy has been, if anything, moderate, at least in developed countries; see, e.g., Dell et al. (2009, 2012). We first calibrate production by disregarding climate damages.In the second step, we calibrate the damage specification.

**Capital Shocks** We set annual volatility of capital diffusion risk to $\sigma_1=\sigma_2=0.02$ matching the observed volatility of consumption or output, e.g., Wachter (2013). We discuss the influence of the *instantaneous correlation* between the two capital stocks in Section 5 and start with a benchmark value of $\rho_{12}=0$, which is also assumed by Cochrane et al. (2007) for an endowment economy. Notice however that there is still comovement between the capital stocks since there are common Poisson shocks affecting the dynamics of the two capital stocks.

We assume that the recovery rates, $Z_i=1-\ell_i$, $i\in\{e,c\}$, have power distributions over $(0,1)$ with parameters $\alpha_i>0$, i.e., the jump size distribution is determined by the density function $\zeta_i(Z_i)=\alpha_i Z_i^{\alpha_i-1}$, $Z_i\in(0,1)$ (see Pindyck and Wang (2013)). This specification is

analytically tractable and the $n^{\text{th}}$ moment of the recovery rate is given by $\mathbb{E}[Z_i^n] = \frac{\alpha_i}{\alpha_i+n}$. To calibrate the macroeconomic jump-size distribution, we follow Barro and Jin (2011) and define a disaster as an event destroying more than $\overline{\ell}_e = 10\%$ of GDP or aggregate consumption. They use historical consumption data to estimate an annual disaster probability of 0.038 and an average consumption loss of 20% when a disaster occurs, i.e., $\mathbb{E}[\ell_e|\ell_e > \overline{\ell}_e] = 0.2$, and $\lambda_e \int_0^{1-\overline{\ell}_e} \zeta_e(Z_e)\mathrm{d}Z_e = 0.038$. This system of equations can be solved to give $\alpha_e = 8$ and $\lambda_e = 0.088$.

**Production and Energy Costs** If we disregard the effects of climate change, the optimal SCC is zero and optimal energy use implies a linear production function $Y_n = A_n^* K_n$, where productivity is given by

$$A_n^* = A_n^{\frac{1}{1-\eta_n}} \left(\frac{\eta_n}{b_n}\right)^{\frac{\eta_n}{1-\eta_n}}. \tag{4.1}$$

To calibrate time preference, risk aversion, adjustment costs and total factor productivity, we use a special case of our model with an aggregate capital stock (see Appendix D). Following Pindyck and Wang (2013), we choose these parameters such that the model generates the following output: a real expected growth rate of consumption of 2%, an average consumption fraction of GDP of 75%, an initial risk-free interest rate of $r_0^f = 0.8\%$ per annum, an average equity premium of 6.3% per annum, and a Tobin'Q of 1.5. We can use this to back out and calibrate a time-preference rate of $\delta = 0.05$ per annum, a degree of relative risk aversion of $\gamma = 5.288$, adjustment cost parameters of $\phi_1 = \phi_2 = 18.12$, and total factor productivities of $A_1^* = A_2^* = 0.1$.[11]

Following van den Bremer and van der Ploeg (2019), we use energy shares $\eta_i = 0.066$ and set the cost of fossil fuel at $b_2 = \$540/\text{tC}$. We use a significantly higher price of green energy, i.e., $b_1 = \$810/\text{etC}$, which is in line with production costs in developed countries such as Germany. Solving (4.1) for $A_i$ yields the sector-specific productivities $A_1 = 0.851$ and $A_2 = 0.828$. Finally, we choose the reallocation cost parameter $\kappa = 1$ such that the model-predicted optimal global average temperature increase is approximately 4°C after 200 years, which is in line with the optimal temperature evolution in the latest version of DICE; see Nordhaus (2017).

[11] We do this by solving the non-linear system of equations (D.1)-(D.5).

## 4.2 Damage Specifications

To compare the effects of different damage specifications on financial markets and the real economy, we consider three different damage specifications:

[Table 2 about here.]

**Level Impact (L–I)** The standard damage function in DICE is inverse quadratic. Nordhaus (2017) uses the parametrization $\Lambda(T) = \frac{1}{1+\theta_i T^2}$ and calibrates the damage function so that damages at 3°C are 2.08% of pre-damages output. This gives $\theta_i = 0.00236$.

**Disaster Impact (D–I)** Karydas and Xepapadeas (2019) collect data on climate-related events for 42 countries over the period from 1911 to 2015.[12] Following the methodology of Loayza et al. (2012), they estimate climate-related disaster probabilities and magnitudes. Their model involves time-varying temperature disaster risk where the disaster intensity follows a mean-reversion process whose long-term mean is linear in temperature, $\overline{\lambda}_c(T) = \overline{\lambda}_{c0} + \overline{\lambda}_{c1} T$. Abstracting from mean reversion, we set $\lambda_c(T) = \lambda_{c0} + \lambda_{c1} T$. with $\lambda_{c0} = 0.003$ and $\lambda_{c1} = 0.096$. This is approximately the probability that a disaster hits within the period of a year. Karydas and Xepapadeas (2019) also report a mean magnitude of $\mathbb{E}[\ell_c] = 1.5\%$ of climate-related disasters. Using a power distribution for the recovery rate $Z_c$ yields the coefficient $\alpha_c = 65.67$.

**Growth Rate Impact (G–I)** We also allow climate damages to affect the growth rate of capital or, equivalently, the depreciation rate. To allow a meaningful comparison with climate disaster risk, we calibrate the damage parameters $\xi_n$ such that the growth rate impact equals the expected climate disaster impact. Therefore, we set $\xi_n = \lambda_{c1}\mathbb{E}[\ell_c]$, which gives $\xi_n = 0.00144$.

## 4.3 Climate Model

[Figure 1 about here.]

[12] They use a database called the international disasters database EM-DAT, which is available at https://www.emdat.be/

**Carbon Emissions** We calibrate the emission intensity per unit of fossil fuel $\nu$ such that under the business-as-usual (BAU) scenario, the model matches the BAU carbon emissions in DICE-2016R. We set $\nu(t, K_1, K_2) = \frac{p(t)}{K_1+K_2}$, where $p(t) = p_0 + p_1 t + p_2 t^2$. A least-squares fit yields $p_0 = 11.03$, $p_1 = 0.1979$, and $p_2 = -8.554 \times 10^{-4}$. Carbon emissions are thus given by $\varepsilon_t = p(t) S_t f_{2t}$.This calibration ensures that carbon emissions are zero if the dirty capital stock is not used and production of dirty goods is zero. The emission intensity tends to decrease over time as in DICE-2016R. Panel (a) of Figure 1 depicts the calibration of the carbon emissions and shows that the model is well in line with the latest version of DICE, see Nordhaus (2017). Panel (b) depicts the expected path of the normalized emission intensity per unit of fossil fuel use, $\mathbb{E}[\nu_t]/\nu_0$, under BAU.

**TCRE** Recent studies estimate a transient climate response to cumulative carbon emissions of 0.8 to 2.4°C/TtC; see, e.g., Allen et al. (2009), Matthews et al. (2009, 2018). The latest version of DICE involves a complex climate module consisting of three carbon layers and two temperature layers. However, its climate module can be approximated by a TCRE of $\beta_1 = 1.8$°C/TtC, which is in line with the above mentioned estimates, see Panel (c) of Figure 1.

# 5 Abatement and Diversification Motives

## 5.1 Effects of Need to Abate on Full Diversification

Since damages resulting from climate change increase in temperature, the indirect utility function $J$ decreases in temperature, $\frac{\partial J}{\partial T} < 0$. By contrast, the effect of the share of dirty capital on indirect utility is non-monotone. As $S$ measures how carbon-intensive the economy is, a higher value of $S$ indicates that there are more carbon dioxide emissions amplifying climate change. This argument suggests that $J$ decreases in $S$. However, the share of dirty capital also determines the volatility of the total stock of capital $K$ which is a convex quadratic function of $S$.[13] More precisely, the total capital volatility equals $\sigma_1$ and $\sigma_2$ at the polar cases, $S = 0$ and $S = 1$, respectively, but takes its minimum value at

$$S^* = \frac{\sigma_1^2 - \sigma_1 \sigma_2 \rho_{12}}{\sigma_1^2 + \sigma_2^2 - 2\sigma_1 \sigma_2 \rho_{12}}. \tag{5.1}$$

[13]This property also holds in the endowment economy analyzed by Cochrane et al. (2007).

It is thus lower for intermediate values of $S$ as the economy is then diversified between the two capital stocks. In particular, if both capital stocks are equally volatile, $\sigma_1 = \sigma_2$, total capital volatility takes its minimum value at $S^* = 1/2$, i.e., if both capital stocks are of the same size. This corresponds to full diversification. We emphasize that with climate change it is not optimal to fully diversify. The optimal level of diversification is independent of the instantaneous correlation between the two capital stocks. However, the variance of the total capital stock is linear in the correlation coefficient, $\|\sigma_k(S^*)\| = \frac{1}{2}\sigma_1^2(1 + \rho_{12})$.[14] Hence, the magnitude of the diversification effect is less pronounced for high values of the correlation coefficient.

Consequently, there are two opposing effects of the share of dirty capital on indirect utility. First, dirty capital causes a negative externality that diminishes output. Therefore, the agent seeks to reduce the share of dirty capital in order to reduce carbon dioxide emissions. We refer to this motive as the *abatement motive*. Second, the agent is risk-averse and thus dislikes volatility. Therefore, the agent also seeks to reduce total capital volatility which is driven by the share of dirty capital. We refer to this motive as the *diversification motive*.

At $S = S^*$, total capital volatility reaches its minimum value. By contrast, for high *and* low values of $S$ the economy is poorly diversified. Since initially dirty capital dominates the capital stock, the diversification motive accelerates climate action until full diversification is reached. At this level, abatement and diversification become conflicting targets and the transition to a low-carbon economy is thus slowed down. Nevertheless, the economy does not stop at the optimal diversification level and the overall optimal level of $S$ lies below $S^*$, i.e., below full diversification. Note that in a setting with externalities the dirty capital stock is typically kept in operation, forever.

The question arises whether the abatement motive or the diversification motive dominates and by how much the abatement motive shifts the optimal level below $S^*$. The answer to this question critically depends on the strength of the damage specification and the instantaneous correlation between the two capital stocks. Especially for low correlation and moderate damages, the abatement motive is significantly dampened by the diversification motive. On the other hand, even in a hypothetical model without damages from climate change, the diversification motive incentivizes the agent to reallocate from the green to the dirty capital stock until

[14] $\sigma_k$ denotes the 3-dimensional volatility vector of the capital stock, see (A.9) in Appendix A. $\|\cdot\|$ denotes the Euclidean norm.

the full diversification $S^*$ is reached. We will explore the strength of the different motives for our different calibrations of our integrated assessment model of economy and the climate.

## 5.2 Policy Simulation Results

Here we highlight the parameters that drive the abatement and diversification motives. To answer the question which motive dominates, we analyze the effect of the strength of the damage specification and of the instantaneous correlation between the two capital stocks. To disentangle both motives, we also consider hypothetical scenarios without damages from climate change. We assume that the initial share of dirty capital is 94% to reflect that due to the various types of investment adjustment and relocation costs the world economy is currently in an undiversified state even when climate policy is not implemented. Initially, there is thus too much of the dirty and too little of the green capital stock. In the absence of climate policy, this share will drop to 50%. With climate policy this share will drop to below 50%.

**Effects of Correlation between the Two Sectors**

[Figure 2 about here.]

The correlation between asset returns plays a crucial role for the optimal asset allocation and, in turn, for asset pricing. This section thus explores the role of the correlation coefficient $\rho_{12}$ between the diffusive shocks to the capital stocks. Figure 2 depicts the optimal evolution of the share of dirty capital for various combinations of the correlation coefficient and for the three damage specifications, level impact (1st column), disaster impact (2nd column), and growth rate impact (3rd column) until the year 2200. Black lines (⋯⋯, ——) shows results for the benchmark case with $\rho_{12} = 0$. Gray lines (⋯⋯, ——) show results for $\rho_{12} = 0.5$. Light lines (⋯⋯, ——) depict the results for $\rho_{12} = -0.5$. We emphasize that the correlation between the two capital stocks and, in turn, between asset prices is significantly driven by macroeconomic disasters. Since both capital stocks suffer common macroeconomic shocks via $N^e$, the true correlation between the capital stocks is significantly higher than $\rho$ indicates. Our numerical simulations show that the true correlation is higher than 90% for all cases under consideration. Dotted lines depict the results for hypothetical scenarios without damages from climate change.[15] In

[15]This is different from the BAU scenario where there are damages from climate change, but they are not corrected for by the policy makers.

these scenarios, there is no benefit from climate action. Therefore, only the diversification motive matters and the agent reallocates capital from the green to the dirty stock until full diversification, $S^* = 50\%$, is eventually reached.

If climate damages are internalized by policy makers, the abatement motive matters. In turn, the share of dirty capital stabilizes at a social optimum below full diversification, $S^* = 50\%$. With zero correlation (·····,——), the optimal share of dirty capital stabilizes between 20% and 30% depending on the damage specification. Crucially, it does not go to zero, as a positive amount of dirty capital is kept for diversification purposes. The differences between the dotted and solid lines thus result from the abatement motive, i.e., from the benefits of combating global warming.

A negative correlation coefficient (·····, ——) amplifies the diversification motive. Therefore, the agent implements a strategy leading to a faster transition to full diversification of $S^* = 50\%$. In the short run, this effect accelerates the decarbonization of the economy, but in the long-run the opposite is true, see Panels a1)-a3) of Figure 2. The agent wants to keep a higher share of dirty capital to benefit from diversification. In turn, the transition is slowed down and ends at a higher steady-state level for the share of dirty capital compared to the benchmark case with zero correlation. In other words, there is less climate action in the long-run if the potential effects from diversification are more pronounced.

For a positive correlation coefficient, the diversification motive is less important, which can be seen from the gray dotted lines (·····). This implies that in the short run, transition from a carbon-intensive to a carbon-free economy is significantly slowed down. In the long-run, however, the abatement motive dominates and the share of dirty assets stabilizes at lower levels (——). Consequently, the speed of transition to a decarbonized economy is significantly effected by the sign and size of the correlation coefficient between the green and dirty capital stock.

**Effects of Different Damage Specifications**

[Figure 3 about here.]

[Table 3 about here.]

Figure 3 depicts the influence of the damage specification on the optimal evolution of the share of dirty capital and global average temperature. The black dotted lines (·····) show the results

for a hypothetical scenario where climate change does not generate economic damages. In this scenario, only the diversification motive matters. If economic damages from climate change are pronounced, the abatement motive comes into play and the optimal level of the share of dirty capital shifts down to a social optimum below $S^* = 50\%$. The black solid lines (—) show the results for the damage parameters that are calibrated as in Section 4. The gray lines (—) depict results with damage parameters that are twice as high as in the benchmark calibration. The light lines (—) show results with damage parameters that are three times higher than those from the benchmark calibration. Table 3 summarizes the damage parameters that are used in Figure 3. It can be seen that for higher damage parameters the abatement motive becomes more pronounced and the diversification motive loses its importance. For sufficiently high damages, the dirty capital stock vanishes and production of carbon-intensive goods ceases. This increases the volatility of total capital, but the benefits from abatement eventually dominate the benefits from diversification. Doubling or tripling the damage parameter has a huge influence on both the growth rate and the disaster impact. The effect for the level impact is however less pronounced.

# 6 Equilibrium Asset Prices

Here, we price both the green and dirty assets in the economy. We first derive the stochastic discount factor of our economy and then provide equilibrium representations of the risk premia as well as of the risk-free rate.

## 6.1 Dynamics of the Stochastic Discount Factor

The information about the current value of future (uncertain) cash flows is summarized in the stochastic discount factor or SDF (also known as state-price deflator or pricing kernel). If the SDF is known, we can calculate today's price of any given cash-flow stream. It thus generalizes standard discount factor ideas.[16]

[16] See, e.g., Cochrane (2005), pp. 6ff.

Duffie and Epstein (1992a) and Duffie and Skiadas (1994) show that for continuous-time recursive utility the SDF has the representation

$$H_s = \exp\left(\int_0^s f_J(C_u, J_u)\, du\right) f_C(C_s, J_s), \tag{6.1}$$

where $J_s$ denotes the time-$s$ value of the indirect utility function. Applying Ito's lemma to (6.1) yields the following dynamics[17]

$$\frac{\mathrm{d}H}{H_-} = \frac{\mathrm{d}f_c(C_-, J_-)}{f_c(C_-, J_-)} + f_J(C, J)\mathrm{d}t, \tag{6.2}$$

where subscripts of $f$ denote partial derivatives and $J$ denotes the indirect utility function whose closed-form representation is given in Proposition 3.1. Although the dynamics of the SDF have the compact representation (6.2), determining the explicit form involves several auxiliary calculations that can be found in Appendix B.1. The dynamics of the SDF contain several pieces of relevant information about key variables of the economy: its drift equals the equilibrium risk-free interest rate (with a negative sign) and the coefficient in front of the Brownian shocks contains the market prices of diffusive risk, see Proposition 6.1 below.

**Proposition 6.1** (Equilibrium)**.** *Let $\sigma_k$ be the three-dimensional volatility vector of the total stock of capital, see (A.9), and $\sigma_g$ be the three-dimensional volatility vector of $G$, see (B.1). Let $\mu_c$ and $\sigma_c$ denote the drift rate and the three-dimensional volatility vector of optimal consumption, respectively, see (B.3) and (B.4). The stochastic discount factor follows the dynamics*

$$\frac{\mathrm{d}H}{H_-} = -r^f \mathrm{d}t + \Theta_W^\top \mathrm{d}W + \sum_{i\in\{e,c\}} \big((1-\ell_i)^{-\gamma} - 1\big)\mathrm{d}N_i - \Theta_N \mathrm{d}t$$

*with $W = (W_1, W_2, W_3)^\top$. The equilibrium risk-free rate $r^f$ is given by*

$$r_t^f = \underbrace{\delta + \mu_c(t, S_t, T_t) - \gamma\|\sigma_c(t, S_t, T_t)\|^2}_{\textit{standard diffusion risk}} \underbrace{- \sum_{i\in\{e,c\}} \lambda_i(T_t)\mathbb{E}_t[\ell_i(1-\ell_i)^{-\gamma}]}_{\textit{disaster risk}} \tag{6.3}$$
$$\underbrace{- \langle \sigma_g(t, S_t, T_t) + (\gamma-1)\sigma_c(t, S_t, T_t), \sigma_k(S_t) - \sigma_c(t, S_t, T_t)\rangle}_{\textit{temperature diffusion risk}}$$

[17] Again we drop all time dependencies. The notation _ is short for $t-$, i.e., the left limit at time $t$. We emphasize that for $\mathrm{d}t$ terms it does not matter whether we take left limits, since integrands of Lebesgue integrals can be changed on zero sets and the jumps of our point process constitute a zero set w.r.t. the Lebesgue measure.

*where $\|\cdot\|$ denotes the Euclidean norm and $\langle\cdot,\cdot\rangle$ the scalar product. The market price of diffusion risk and the market price of jump risk are given by*

$$\begin{aligned}\Theta_{Wt} = & \underbrace{-\gamma\sigma_k(S_t)}_{\text{standard risk}} + \underbrace{\sigma_g(t,S_t,T_t)+\sigma_k(S_t)-\sigma_c(t,S_t,T_t)}_{\text{temperature risk}},\\ \Theta_{Nt} = & \sum_{i\in\{e,c\}}\lambda_i(T_t)\mathbb{E}[(1-\ell_i)^{-\gamma}-1].\end{aligned}$$

Proposition 6.1 constitutes a similar decomposition of the risk-free interest rate that as in Barro (2006, 2009), Pindyck and Wang (2013), and Wachter (2013), among others. The first two terms in equation (6.3) also arise in deterministic models: the time preference rate $\delta$ captures preferences about the timing of consumption. If $\delta$ is high, there are strong preferences for early consumption and one would thus like to borrow. Since, in equilibrium, the risk-free asset is in zero net supply, the risk-free rate must increase to counter this. Besides, the risk-free rate increases in the expected growth rate of consumption $\mu_c(t,S_t,T_t)$ (C.1) since it is desirable to smooth consumption. Notice that the EIS is one and thus the growth rate is multiplied by one.

The third term involves $\gamma\|\sigma_c(t,S_t,T_t)\|^2$ in equation (6.3). This represents the motive for precautionary savings in response to diffusion risk. In turn, the interest rate has to go down to keep the risk-free asset in zero net supply. The expected consumption growth rate and its volatility depend non-linearly on both the temperature and the dirty capital share, whereby the result is more involved and qualitatively different from one-tree endowment economies.

The fourth term in equation (6.3) is $\sum_i \lambda_i(T_t)\mathbb{E}_t[\ell_i(1-\ell_i)^{-\gamma}]$. This term reflects precautionary savings in response to disaster risk. As for standard diffusion risk, these terms reduce the interest rate to keep the risk-free asset is in zero net supply. The greater the risk aversion, the greater is this effect, see also the extensive discussion in Wachter (2013). Notice that a novel feature is that the jump intensity for climate disaster risk $\lambda_c$ increases in temperature and thus higher temperatures reduce the risk-free interest rate.

The last term in equation (6.3) is $\langle\sigma_g(t,S_t,T_t)+(\gamma-1)\sigma_c(t,S_t,T_t),\sigma_k(S_t)-\sigma_c(t,S_t,T_t)\rangle$. This captures the interdependence between capital, consumption, and the indirect utility. Compared to Cochrane et al. (2007) this term is new and results from the inability to hedge temperature shocks, i.e., it represents precautionary savings for uninsurable temperature risk. We emphasize that these components depend on the relevant state variables in a highly nonlinear manner. We

calculate these variables numerically using finite differences, see Appendix C.2. An extensive discussion of theses effects in a calibrated model is given in Section 6.3.

## 6.2 Pricing Dividend Claims

Using the representation of the pricing kernel, we can now calculate the ex-dividend price $P_n$ of both assets in the economy. For the dividend stream $D_n$, the time-$t$ price of asset $n$ equals

$$P_{nt} = \mathbb{E}_t\Big[\int_t^\infty \frac{H_s}{H_t} D_{ns}\mathrm{d}s\Big]. \tag{6.4}$$

We denote the price-dividend ratio of asset $n$ by $\Omega_n = P_n/D_n$. Its equilibrium expected excess return can be interpreted as the risk premium of the asset. It is formally given by the sum of its expected ex-dividend stock return, $\mu_{P_n}$, plus its dividend yield, $\Omega_n^{-1}$, minus the risk-free interest rate, $r^f$,

$$\mathrm{rp}_{nt} = \mu_{P_n t} + \Omega_{nt}^{-1} - r_t^f. \tag{6.5}$$

It can be shown that the price-dividend ratio $\Omega_n = P_n/D_n$ satisfies the parabolic partial differential equation (B.9) which we solve numerically. The technical details are given in Appendices B.3 and B.4.

## 6.3 Drivers of the Risk-Free Rates and of the Risk Premiums

[Table 4 about here.]

Table 4 reports the decomposition of the risk-free rate into its state-dependent parts for the year 2100. The qualitative behavior is robust over time and similar for other years. In contrast to Karydas and Xepapadeas (2019), the drift rate of the consumption process $\mu_c$ and its volatility $\sigma_c$ are endogenous. They depend on temperature and the share of dirty capital.

It can be seen that expected consumption growth $\mu_c$ decreases in both temperature and the share of dirty capital. The negative influence of temperatures reflects the impact of climate change on output and is in line with other integrated assessment models. The negative influence of the share of dirty capital on consumption growth can be explained as follows. First, optimal fossil fuel decreases in the share of dirty capital. Since fossil fuel is a production factor, output

is reduced and thus a high share of dirty capital negatively affects economic growth. Second, if the share of dirty capital is large, the agent reallocates capital at a higher rate which leads to higher capital adjustment costs and thus reduces the consumption growth rate. Consequently, the risk-free rate decreases as well. Additionally, there is precautionary savings for uninsurable climate risks represented by the term $\langle \sigma_g, \sigma_\chi \rangle$. This term increases in temperature, but its absolute size turns out to be almost negligible.

[Figure 4 about here.]

The consumption volatility is also state dependent. While the effect of temperature on the precautionary-savings term $\gamma \|\sigma_c\|^2$ is small, the share of dirty capital has a significant influence on the equilibrium risk-free rate. The latter result stems from a diversification argument as in Cochrane et al. (2007). In line with this literature, the precautionary savings term $\gamma \|\sigma_c\|^2$ depends in a non-monotone way on $S$. Recall that the total capital volatility reaches its minimum value at the expression given in (5.1). Since we have $\rho_{12} = 0$ and $\sigma_1 = \sigma_2$, the term attains its minimum value at $S = 1/2$. Therefore, diversifying across the green and dirty capital stock reduces the volatility of the total capital stock and this effect carries over to aggregate consumption since

$$\gamma \|\sigma_c\|^2 = \gamma \|\sigma_k\|^2 + \gamma \langle \sigma_\chi, \sigma_k \rangle.$$

This explains the non-monotonic behavior of the consumption volatility and, in turn, the non-monotonic relation between the share of dirty capital and the equilibrium risk-free rate.

Figure 4 depicts how several relevant quantities depend on temperature and the share of dirty capital. Panels a) and b) show that the Tobin's Q for both the green and the dirty sector decreases in temperature. The opposite is true for the book-to-market ratio. This implies that for a fixed amount of capital the market value decreases in temperature, both for the green and dirty asset. Panel a) shows that the Tobin's Q of the green asset increases in the share of dirty capital. Therefore, for a fixed amount of capital the green asset has a higher market value if the economy is more carbon intensive. Panel b) indicates that the opposite is true for the carbon-emitting asset.

Panel c) shows the equilibrium risk-free rate whose behavior has been discussed above. Notice however that for low temperatures, the effect of the share of dirty capital on the risk-free rate is ambiguous which is due to the trade-off between the diversification and the abatement motives.

[Table 5 about here.]

Panels d) and e) depict the risk premia of the green and dirty asset, respectively. For the year 2100, Table 5 reports decompositions into the relevant components. Here $\mu_{P_n}$ denotes the expected ex-dividend stock return and $\Omega_n^{-1}$ the dividend yield of asset $n$. It turns out that the green risk premium $\text{rp}_1$ increases in both temperature and the share of dirty capital. The share of dirty capital has a significant positive influence on the risk premium while the effect of temperature is less pronounced. The same holds true for the expected ex-dividend green stock return $\mu_{P_1}$ which sharply increases in the share of dirty capital. Notice that the opposite is true for its dividend yield $\Omega_n^{-1}$. If the share of dirty capital is high, the green stock pays fewer dividends. When the transition to a low-carbon economy is completed, the green asset pays higher dividends. This is also in line with the positive relation between the share of dirty capital and the green Tobin's $Q$.

Panels d) and e) in Figure 4 show how the dirty and the green risk premium vary with temperature for given shares of dirty capital.[18] To understand the results, first notice that our agent has the option to convert dirty into green capital at some adjustment costs. If we disregard this option for the moment, then the risk premium of the dirty and green sector is inversely related to its share, $S$ and $1 - S$, respectively. In an economy with damages from climate change, these premia additionally increase in temperature since higher temperatures make the economy riskier. If we also take the option to convert dirty capital into account, then the value of the dirty asset involves the value of this option. For economies with high shares of dirty capital and currently low temperatures, the option value is relatively high and thus the risk premium of the dirty asset is low. This can be seen on the left-hand side of Panel e) in Figure 4. If the temperature is higher, then keeping a higher share of dirty capital is riskier and thus the risk premium of the dirty asset increases (dark line, ——). The opposite is true for economies with equal shares of both capital stocks. In this case, the option to convert gains more value than is destroyed by higher temperatures, and thus the risk premium decreases (gray line, ——). Notice that compared to a model without the option to convert, the existence of an option to convert also reverses the order of the green risk premium in Panel d). This is because the dirty and clean assets are priced in general equilibrium, i.e., changes in the valuation of the dirty asset also feeds back into the valuation of the green asset.

[18] What we are looking is different from the carbon risk associated with stranded assets, e.g., Bolton and Kacperczyk (2020).

# 7 Optimal Policy Simulations

Here we present our our optimal policy simulation results for the model of Section 2. We determine optimal carbon-dioxide emissions and consumption and simulate the evolution of global output, the relevant state variables, and the asset returns over the next 100 years. The columns of Figures 6 and 7 show results for the three damage specifications (L–I), (D–I), and (G–I), respectively. Unless otherwise stated, we use our benchmark calibration from Section 4, which is summarized in Table 1. Optimal paths are depicted by solid lines (——) and BAU paths by dotted lines (·····). Dashed lines (- - -) show 5% and 95% quantiles of the optimal solution.

## 7.1 State-Space Solutions

Before analyzing simulated paths, we discuss the influence of the state variables on the optimal decisions and asset returns. From this, we can derive intuition for the influence of the share of dirty capital and temperature on the optimal controls and understand the economic forces at play. In particular, we discuss how climate change affects the interest rate and asset returns. All the results presented in this section are for the benchmark calibration for the year 2100 and for the level impact (L–I). The policy functions behave in a qualitatively similar manner for other years and for our alternative parametrizations of damages. The qualitative behavior of the asset returns is hardly affected by the choice of the damage specification. The lines in Figure 5 represent various levels of the capital share: The dark lines (——) depict $S = 0.95$, the gray lines (——) refers to $S = 0.5$, and the light lines (——) to $S = 0.05$. The horizontal axis depicts the temperature in the range from 0°C to 5°C.

[Figure 5 about here.]

Panel a) of Figure 5 shows that the optimal investment in the green capital stock decreases in the share of dirty capital $S$, whereas Panel b) shows that the opposite is true for the investment in the dirty capital stock. This can be explained by the diversification argument from Section 3. If damages are moderate (as for the DICE damage specification), the economy retains a certain level of dirty capital to reach an optimal level of diversification. Therefore, the agent invests more in the green capital stock if the share of dirty capital is high and more in the dirty capital stock if this share is low. Panel c) shows that the optimal consumption strategy hardly depends

on the share of dirty capital. This reflects the agent's motive for consumption smoothing. Instead of adjusting the consumption rate in response to the changes in the share of dirty capital, the economy increases the green investment ratio and decreases the dirty investment ratio to smooth consumption. Panel d) depicts fossil fuel use relative to the respective capital stock, which does not vary very much with the share of dirty capital. The corresponding ratio for green energy, $F_1/K_1$, does not depend on the share of dirty capital at all.[19] Panel e) depicts carbon emissions and shows that in absolute terms fossil fuel use decreases both in the share of dirty capital and temperature.

Panel f) depicts the optimal carbon tax as a fraction of total capital. It shows that the optimal carbon tax sharply increases in temperature and increases only moderately in the share of dirty assets. In recent years, a literature has evolved that derives simple formulas for the optimal social cost of carbon in deterministic environments, e.g., Nordhaus (1991), Golosov et al. (2014), Rezai and van der Ploeg (2016), van den Bijgaart et al. (2016), van der Ploeg and Rezai (2019), and Hambel et al. (2018). This strand of literature considers analytical models and generates social costs of carbon that do not depend on temperature.[20] By contrast, our framework explicitly models stochastic climate risks and uses a convex damage function, which yields temperature-dependent carbon taxes and optimal controls. Consequently, society reacts to increasing climate risks by raising carbon taxes and thus to more pronounced carbon abatement for higher temperatures.[21]

## 7.2 Effects of Climate Policy on the Economy

[Figure 6 about here.]

Figure 6 depicts the optimal evolution of the real economy under three different damage specifications. It shows that the qualitative behavior is similar for all specifications. Comparing the second column to the third column indicates that there are only small differences between

[19] See the first-order condition (3.5).

[20] The reason is that the concavity of the logarithmic Arrhenius' law linking temperature to the atmospheric stock of carbon is (more or less) exactly offset by the convexity of the function relating the damage ratio to temperature, see Golosov et al. (2014). For more convex damage ratios, the ratio of the optimal SCC to GDP increases in temperature (e.g., Rezai and van der Ploeg (2016)).

[21] Notice that for the damage specifications (D–I) and (G–I), damages are linear in temperature rather than convex. In turn, the policy functions are almost independent of temperature as in the above mentioned strand of literature. The corresponding figures are available upon request.

the growth rate impact and the disaster impact, which is in part due to how we calibrate the growth rate impact.

Panels a1)-a3) depict the time paths of output. As a result of climate action, the optimal evolutions exhibit a higher economic growth compared to the BAU evolution since some of the climate damages are avoided. This is true for all damage specifications. For the growth rate and the disaster impact, the climate damages are more pronounced and economic growth is significantly dampened compared to the level impact.

Panels b1)-b3) depict the relative consumption rate, expressed as a fraction of output. The optimal relative consumption rate is in a narrow range between 75% to 76%. Notice that the confidence band of the optimal consumption rate is significantly wider for (L–I) than for the other specifications. This is because society responds with a more temperature-sensitive consumption strategy under level impact damages. In particular, for the BAU case, the optimal consumption rate sharply increases for high temperatures around 4°C. A potential explanation is the convexity of the damage function, which leads to a higher sensitivity to atmospheric temperature. For the other damage specifications which are linear in temperature, optimal consumption exhibit small variation across states. In the BAU case, optimal consumption is almost constant.

[Figure 7 about here.]

Panels c1)-c3) depict the evolution of the carbon dioxide emissions that are significantly dampened compared to the BAU case. In general, the variation of optimal emissions is low. As discussed in the previous section, optimal emissions are mainly driven by the share of dirty capital, while the influence of temperature is relatively weak. The small variation of the optimal carbon dioxide emissions thus follows from the small variation in $S$ depicted in Panels d1)-d3). The evolution of the share of dirty capital is crucial for understanding the interaction between the diversification and the abatement motive. If we disregard damages from climate change, the share of dirty assets will eventually stabilize at $S^* = 50\%$. On the other hand, if society recognizes climate change and fights global warming, the share of dirty capital is reduced to approximately 30%. However, dirty capital does not vanish completely since some positive amount is kept to satisfy the diversification motive. In this sense, the diversification motive eventually reduces climate action and this result is robust across all damage specifications.[22]

[22]If all three damage specifications impact simultaneously, the combined response is more than the sum of the individual policy reactions, and the share of dirty capital eventually goes to zero. The reason is that the

### 7.3 Effects of Climate Policy on Asset Prices

Figure 7 complements the results presented in Figure 6 and presents the optimal evolution of quantities relevant for asset pricing. Panels a1)-a3) depict the evolution of the green Tobin's Q, whereas Panels b1)-b3) show the evolution of the dirty one. In the optimum, the green Tobin's Q decreases over time, but the dirty Tobin's Q remains always smaller than the green Tobin's Q. For the disaster and the growth rate impact, the green Q stabilize around 1.5, while for the level impact the green Tobin's Q continues to decrease below that level.

Panels c1)-c3) show the evolution of the equilibrium risk-free interest rate. It decreases for all scenarios including BAU, since over time the expected damages from global warming become more pronounced and households respond with higher precautionary savings. This effect is much stronger under BAU, since then climate damages are more severe. By contrast, if carbon is optimally priced, the downward trend of the risk-free interest rate is less pronounced.

Panels d1)-d3) show the evolution of the green risk premium, whereas Panels e1)-e3) depicts the evolution of the dirty risk premium. As discussed in the previous section, the dirty risk premium depends on the state variables $S$ and $T$ in a non-linear way. This might explain the "snake-shaped" evolution of the dirty risk premium over time for the level and growth rate impact. For the disaster impact, the risk premiums are higher and increasing. This is triggered by the additional Poisson shock $N_e$ which gives rise to an extra component in the risk premium, as seen in Proposition 6.1. Since the jump intensity increases in temperature and global warming becomes more significant over time, the relative importance of the extra component sharply increases under BAU. This reflects the fact that asset holders must be compensated for the increasing climate risks.

## 8 Conclusion

Our main concern has been the interplay between climate action and financial considerations. Since the market wants to hold diversified asset holdings, the transition towards an emissions-free economy is affected by diversification motives. We have shown that diversification and climate action are initially complementary goals, since agents want to decarbonize the economy and hold a balanced portfolio of carbon-free and carbon-intensive assets. At a certain point,

more damage global warming does the more likely it is we get into more damaging regions. In other words, the externalities reinforce each other. These results are available upon request.

however, the two goals become conflicting and a trade-off arises. This is because environmental considerations incentivize the agent to further reduce the dirty capital share, but in turn the agent's assets holdings become less diversified. Hence, climate policy is frustrated by the need to diversify financial asset holdings. Furthermore, it is usually not optimal to fully close down carbon-intensive sectors as they serve as a hedge in the long run and keeping the carbon-intensive sector open in the short run allows a faster build-up of green assets in the short run. The qualitative implications of these effects are robust and hold for three common approaches to model the adverse effects of climate change on economic activity, the depreciation rate of capital and the risk of macroeconomic disasters, respectively. Only if the impact of climate change on economic activity is significantly more pronounced than suggested by DICE, is it optimal to close down the carbon-intensive sector.

We have also analyzed the dynamics of risk premia and the risk-free rate during the transition towards a low-carbon economy. We show that the existence of potential climate disasters is crucial for finding a significant effect of climate change on asset prices. In the absence of climate disasters, the effect of climate change on asset prices is moderate. From the perspective of policy makers, our findings are challenging. Our results suggest that initially agents should be intrinsically motivated to take climate action, simply to reach diversified asset holdings. Only if policy makers want to speed up the process, they must take extra action. Later in the transition process matters change fundamentally. If policy makers wish to incentivize agents to reduce the carbon-intensive capital stock beyond its optimal share, then they must counter the effects of diversification.

Further research is needed to obtain empirical evidence on how climate policy affects the return on and prices of financial assets, both in sectors that make substantial use of fossil fuel and others that make more use of renewable energy. In particular, evidence is needed on the covariance of macroeconomic shocks, both normal and macroeconomic and climate disaster shocks, hitting the brown and green sectors to assess how important the asset diversification and hedging arguments are that we have analyzed. Finally, future research needs to depart from the socially optimal outcomes for the global economy and consider policy uncertainty and the consequences for stranding of financial assets and the implications for returns and risk premia.[23]

[23] A survey of stranded carbon-intensive assets is provided by van der Ploeg and Rezai (2020).

# References


Ackerman, F., E. A. Stanton, and R. Bueno, 2013, Epstein-Zin utility in DICE: Is risk aversion irrelevant to climate policy?, *Environmental and Resource Economics* 56, 73–84.

Allen, M. R., D. J. Frame, C. Huntingford, C. D. Jones, J. A. Lowe, M. Meinshausen, and N. Meinshausen, 2009, Warming caused by cumulative carbon emissions towards the trillionth tonne, *Nature* 458, 1163–1166.

Bansal, R., D. Kiku, and M. Ochoa, 2017, Price of long-run temperature shifts in capital markets, *Working Paper,* Duke University.

Bansal, R., D. Kiku, and M. Ochoa, 2019, Climate change and growth risks, *Working Paper,* Duke University.

Bansal, R., and A. Yaron, 2004, Risks for the long run: A potential resolution of asset pricing puzzles., *Journal of Finance* 1481–1509.

Barnett, M., W. Brock, and L.P. Hansen, 2020, Pricing uncertainty induced by climate change, *Review of Financial Studies* 33, 1024–1066.

Barro, R. J., 2006, Rare disasters and asset markets in the twentieth century, *Quarterly Journal of Economics* 121, 823–866.

Barro, R. J., 2009, Rare disasters, asset prices, and welfare costs, *American Economic Review* 99, 243–264.

Barro, R. J., and T. Jin, 2011, On the size distribution of macroeconomic disasters, *Econometrica* 79, 1567–1589.

Benzoni, L., P. Collin-Dufresne, and R. Goldstein, 2011, Explaining asset pricing puzzles associated with the 1987 market crash, *Journal of Financial Economics* 101, 552–573.

Bolton, P., and M. Kacperczyk, 2020, Do investors care about carbon risk?, *NBER Working Paper* 26968.

Branger, N., H. Kraft, and C. Meinerding, 2016, The dynamics of crises and the equity premium, *Review of Financial Studies* 29, 232–270.

Bretschger, L., and A. Vinogradova, 2019, Best policy response to environmental shocks: building a stochastic framework, *Journal of Environmental Economics and Management* 97, 23–41.

Cai, Y., and T. S. Lontzek, 2019, The social cost of carbon with economic and climate risks, *Journal of Political Economy* 127, 2684–2734.

Cochrane, J. H., 2005, *Asset pricing* (Princeton University Press).

Cochrane, J. H., F. A. Longstaff, and P. Santa-Clara, 2007, Two trees, *Review of Financial Studies* 21, 347–385.

Crost, B., and C. P. Traeger, 2014, Optimal $CO_2$ mitigation under damage risk valuation, *Nature Climate Change* 4, 631–636.

Daniel, K., R. Litterman, and G. Wagner, 2019, Declining $CO_2$ price paths, *Proceedings of the National Academy of Sciences of the United States of America* 116, 20886–20891.

Dell, M., B. F. Jones, and B. A. Olken, 2009, Temperature and income: Reconciling new cross-sectional and panel estimates, *American Economic Review* 99, 198–204.

Dell, M., B. F. Jones, and B. A. Olken, 2012, Temperature shocks and economic growth: Evidence from the last half century, *American Economic Journal: Macroeconomics* 4, 66–95.

Dietz, S., C. Gollier, and L. Kessler, 2018, The climate beta, *Journal of Environmental Economics and Management* 87, 258–274.

Dietz, S., and F. Venmans, 2019, Cumulative carbon emissions andeconomic policy: In search ofgeneral principles, *Journal of Environmental Economics and Management* 96, 108–129.

Donadelli, M., M. Jueppner, M. Riedel, and C. Schlag, 2017, Temperature shocks and welfare costs, *Journal of Economic Dynamics and Control* 82, 331–355.

Duffie, D., and L. G. Epstein, 1992a, Asset pricing with stochastic differential utility, *Review of Financial Studies* 5, 411–36.

Duffie, D., and L. G. Epstein, 1992b, Stochastic differential utility, *Econometrica* 60, 353–394.

Duffie, D., and C. Skiadas, 1994, Continuous-time asset pricing: A utility gradient approach, *Journal of Mathematical Economics* 23, 107–132.

Epstein, L. G., and S. E. Zin, 1989, Substitution, risk aversion, and the temporal behavior of consumption and asset returns: A theoretical framework, *Econometrica* 57, 937–969.

Golosov, M., J. Hassler, P. Krusell, and A. Tsyvinsky, 2014, Optimal taxes on fossil fuel in general equilibrium, *Econometrica* 82, 41–88.

Hambel, C., H. Kraft, and E. S. Schwartz, 2018, The social cost of carbon in a non-cooperative world, *NBER Working Paper* 24604.

Hassler, J., P. Krusell, C. Olovsson, and M. Reiter, 2020, On the effectiveness of climate policies, *Working Paper,* Stockholm University.

IPCC, 2014, *Fifth Assessment Report of the Intergovernmental Panel on Climate Change* (Cambridge University Press).

Jensen, S., and C. P. Traeger, 2014, Optimal climate change mitigation under long-term growth uncertainty: Stochastic integrated assessment and analytic findings, *European Economic Review* 69, 104–125.

Karydas, C., and A. Xepapadeas, 2019, Climate change financial risks: pricing and portfolio allocation, *Working Paper,* ETH Zurich.

Kreps, D. M., and E. L. Porteus, 1978, Temporal resolution of uncertainty and dynamic choice theory, *Econometrica* 46, 185–200.

Loayza, N. V., E. Olaberra, J. Rigolini, and L Christiaensen, 2012, Natural disasters and growth: going beyond the averages, *World Development* 40, 1317–1336.

Matthews, H. D., N. P. Gillett, P. A. Stott, and K. Zickfeld, 2009, The proportionality of global warming to cumulative carbon emissions, *Nature* 459, 829–832.

Matthews, H. D., K. Zickfeld, R. Knutti, and M. R. Allen, 2018, Focus on cumulative emissions, global carbon budgets and the implications for climate mitigation targets, *Environmental Research Letters* 13, 010201.

Munk, C., and C. Sørensen, 2010, Dynamic asset allocation with stochastic income and interest rates, *Journal of Financial Economics* 96, 433–462.

Nordhaus, W. D., 1991, To slow or not slow: the economics of the greenhouse effect, *Economic Journal* 101, 920–937.

Nordhaus, W. D., 1992, An optimal transition path for controlling greenhouse gases, *Science* 258, 1315–1319.

Nordhaus, W. D., 2017, Revisiting the social cost of carbon, *Proceedings of the National Academy of Sciences* 114, 1518–1523.

Nordhaus, W. D., and P. Sztorc, 2013, DICE 2013R: Introduction and user's manual, *Technical Report,* Yale University.

Pindyck, R. S., and N. Wang, 2013, The economic and policy consequences of catastrophes, *American Economic Journal: Economic Policy* 5, 306–339.

Rezai, A., and F. van der Ploeg, 2016, Intergenerational inequality aversion, growth and the role of damages: Occam's rule for the global carbon tax, *Journal of the Association of Environmental and Resource Economics* 3, 499–522.

Scheffers, B., L. De Meester, T. Bridge, A. Hoffmann, J. Pandolfi, R. Corlett, S. Butchart, P. Pearce-Kelly, K Kovacs, D. Dudgeon1, M. Pacifici, C. Rondinini, W. Foden, T. Martin, C. Mora, D. Bickford, and J. Watson, 2019, The broad footprint of climate change from genes to biomes to people, *Science* 354, 719–732.

Traeger, C., 2019, Ace–analytic climate economy (with temperature and uncertainty), *Working Paper,* University of Oslo.

van den Bijgaart, I., R. Gerlagh, and M. Liski, 2016, International aspects of pollution control, *Journal of Environmental Economics and Management* 77, 75–96.

van den Bremer, T. S., and F. van der Ploeg, 2019, The risk-adjusted carbon price, *Working Paper,* University of Oxford.

van der Ploeg, F., 2018, The safe carbon budget, *Climatic Change* 147, 47–59.

van der Ploeg, F., and A. Rezai, 2019, Simple rules for climate policy and integrated assessment, *Environmental and Resource Economics* 72, 77–108.

van der Ploeg, F., and A. Rezai, 2020, Stranded assets in the transition to a carbon-free economy, *Annual Review of Resource Economics* 12:4, 1–18.

Wachter, J. A., 2013, Can time-varying risk of rare disasters explain aggregate stock market volatility?, *The Journal of Finance* 68, 987–1035.

# A Indirect Utility or Value Function

To solve the Hamilton-Jacobi-Bellman equation (3.1), we first transform it by expressing the decision variables in relative terms and reducing the number of state variables by one. Letting $i_n = I_n/K_n$, $f_n = F_n/K_n$, $r = R/K_1$ denote the relative control variables. The dynamics of the state variables can be rewritten as

$$\begin{aligned}
\mathrm{d}K_1 &= K_{1-}\Big[\Big(i_1 - \frac{1}{2}\phi_1 i_1^2 + r - \frac{1}{2}\kappa r^2 - (\delta_1^k + \xi_1 T)\Big)\mathrm{d}t + \sigma_1 \mathrm{d}W_1 - \big(\ell_e \mathrm{d}N_e + \ell_c \mathrm{d}N_c\big)\Big], \\
\mathrm{d}K_2 &= K_{2-}\Big[\Big(i_2 - \frac{1}{2}\phi_2 i_2^2 - r\frac{K_1}{K_2} - (\delta_2^k + \xi_2 T)\Big)\mathrm{d}t + \sigma_2\Big(\rho_{12}\mathrm{d}W_1 + \sqrt{1-\rho_{12}^2}\mathrm{d}W_2\Big) - \big(\ell_e \mathrm{d}N_e + \ell_c \mathrm{d}N_c\big)\Big], \\
\mathrm{d}T &= \widehat{\beta} f_2 \mathrm{d}t + \sigma_T(T)\mathrm{d}W_3.
\end{aligned}$$

where $\widehat{\beta} = \beta/K_2$. To shorten the notation, we sometimes write $W = (W_1, W_2, W_3)^\top$ and denote the drift of the capital stocks and temperature by $\mu_{K_i}$ and $\mu_T$, respectively. Following Cochrane et al. (2007), we define $K = K_1 + K_2$ and $S = K_2/(K_1 + K_2)$. As the economy decarbonizes, the share $S$ declines. The dynamics of $K$ and $S$ can be calculated using Ito's lemma:

$$\begin{aligned}
\mathrm{d}S &= S(1-S)\Big[\mu_S(i_1, i_2, r, T, S)\mathrm{d}t + (\sigma_2\rho_{12} - \sigma_1)\mathrm{d}W_1 + \sigma_2\sqrt{1-\rho_{12}^2}\mathrm{d}W_2\Big] \\
\mathrm{d}K &= K_-\Big[\mu_K(i_1, i_2, r, T, S)\mathrm{d}t + [(1-S)\sigma_1 + S\sigma_2\rho_{12}]\mathrm{d}W_1 + S\sigma_2\sqrt{1-\rho_{12}^2}\mathrm{d}W_2 - \big(\ell_e \mathrm{d}N_e + \ell_c \mathrm{d}N_c\big)\Big].
\end{aligned}$$

where the drifts are given by

$$\begin{aligned}
\mu_S(i_1, i_2, r, T, S) &= \mu_{K_1} - \mu_{K_2} + S(\sigma_1\sigma_2\rho_{12} - \sigma_2^2) + (1-S)(\sigma_1^2 - \sigma_1\sigma_2\rho_{12}) \\
\mu_K(i_1, i_2, r, T, S) &= (1-S)\mu_{K_1} + S\mu_{K_2}
\end{aligned}$$

We thus solve a modified HJB equation with finite differences in terms of only two $(S, T)$ instead of three state variables $(K_1, K_2, T)$. The following Proposition summarizes our findings.

**Proposition A.1** (Indirect Utility and Optimal Controls)**.** *Suppose $\widehat{\beta} = \widehat{\beta}(t, S, T)$. The indirect utility function (2.5) has the form*

$$J(t, K_1, K_2, T) = \frac{1}{1-\gamma}(K_1 + K_2)^{1-\gamma} G\big(t, T, S(K_1, K_2)\big). \tag{A.1}$$

*where $G$ satisfies a certain HJB equation which is given in (A.8) below. The optimal reallocation strategy is*

$$r = \frac{1}{\kappa}\Big(\frac{G_S}{G_S S + (\gamma-1)G}\Big) \tag{A.2}$$

*and optimal green energy use is*

$$f_1 = \Big(\frac{b_1}{\eta_1 A_1 \Lambda_1(T)}\Big)^{\frac{1}{\eta_1 - 1}}.$$

*The optimal investment strategies and fossil fuel use follow from the following nonlinear system of equations:*

$$\begin{aligned}
&\big[(1-\gamma)G - G_S S\big][1-\phi_1 i_1] \\
&\qquad = \frac{\delta(1-\gamma)G}{(A_1 f_1^{\eta_1}\Lambda_1(T) - i_1 - b_1 f_1)(1-S) + (A_2 f_2^{\eta_2}\Lambda_2(T) - i_2 - b_2 f_2)S} \qquad \text{(A.3)} \\
&\big[(1-\gamma)G + G_S(1-S)\big][1-\phi_2 i_2] \\
&\qquad = \frac{\delta(1-\gamma)G}{(A_1 f_1^{\eta_1}\Lambda_1(T) - i_1 - b_1 f_1)(1-S) + (A_2 f_2^{\eta_2}\Lambda_2(T) - i_2 - b_2 f_2)S} \qquad \text{(A.4)} \\
&\frac{(A_2\eta_2 f_2^{\eta_2-1}\Lambda_2(T) - b_2)S\delta(1-\gamma)G}{(A_1 f_1^{\eta_1}\Lambda_1(T) - i_1 - b_1 f_1)(1-S) + S(A_2 f_2^{\eta_2}\Lambda_2(T) - i_2 - b_2 f_2)} \\
&\qquad = -G_T\beta \qquad \text{(A.5)}
\end{aligned}$$

*The optimal social cost of carbon is*

$$\tau_c = \frac{\vartheta C}{\delta(\gamma-1)}\frac{G_T}{G}, \tag{A.6}$$

*where optimal consumption reads*

$$C = \Big((1-S)[A_1 f_1^{\eta_1}\Lambda_1(T) - i_1 - b_1 f_1] + S[A_2 f_2^{\eta_2}\Lambda_2(T) - i_2 - b_2 f_2]\Big)K. \tag{A.7}$$

*Proof.* Let $i_n = I_n/K_n$, $f_n = F_n/K_n$, $r = R/K_1$ denote the control variables in relative terms. Substituting these relative controls into (3.1) leads to the HJB equation:

$$0 = \sup_{i_1,i_2,f_1,f_2,r}\Big\{\delta(1-\gamma)J\log\Big(\frac{A_1K_1f_1^{\eta_1}\Lambda_1(T) + A_2K_2f_2^{\eta_2}\Lambda_2(T) - i_1K_1 - i_2K_2 - b_1f_1K_1 - b_2f_2K_2}{[(1-\gamma)J]^{\frac{1}{1-\gamma}}}\Big)$$

$$
\begin{aligned}
&+ J_{K_1}K_1\big(i_1 - \frac{1}{2}\phi_1 i_1^2 + r - \frac{1}{2}\kappa r^2 - (\delta_1^k + \xi_1 T)\big) + J_{K_2}K_2\big(i_2 - \frac{1}{2}\phi_2 i_2^2 - r\frac{K_1}{K_2} - (\delta_2^k + \xi_2 T)\big) \\
&+ \frac{1}{2}J_{K_1K_1}K_1^2\sigma_1^2 + \frac{1}{2}J_{K_2K_2}K_2^2\sigma_2^2 + J_{K_1K_2}K_1K_2\sigma_1\sigma_2\rho_{12} + J_T\beta K_2 f_2 + J_{TT}\frac{1}{2}\sigma_T(T)^2 + \\
&+ \lambda_e\mathbb{E}[J(K_1(1-\ell_e), K_2(1-\ell_e), T) - J] + \lambda_c(T)\mathbb{E}[J(K_1(1-\ell_c), K_2(1-\ell_c), T) - J]\Big\}
\end{aligned}
$$

We conjecture that the indirect utility function has the form

$$
J(K_1, K_2, T) = \frac{1}{1-\gamma}(K_1 + K_2)^{1-\gamma}G\big(T, S(K_1, K_2)\big).
$$

The partial derivatives of $S$ are $S_{K_1} = \frac{-S}{K_1+K_2}$, $S_{K_2} = \frac{1-S}{K_1+K_2}$. This specification implies

$$
G(T, S) > 0, \qquad G_T(T, S) > 0.
$$

The relevant partial derivatives of the indirect utility function $J$ are

$$
\begin{aligned}
J_{K_1} &= K^{-\gamma}G + \frac{1}{1-\gamma}K^{1-\gamma}G_S\frac{-S}{K}, \\
J_{K_1K_1} &= -\gamma K^{-\gamma-1}G + 2K^{-\gamma}G_S\frac{-S}{K} + \frac{1}{1-\gamma}K^{1-\gamma}\Big[G_{SS}\frac{S^2}{K^2} + 2G_S\frac{S}{K^2}\Big], \\
J_{K_2} &= K^{-\gamma}G + \frac{1}{1-\gamma}K^{1-\gamma}G_S\frac{1-S}{K}, \\
J_{K_2K_2} &= -\gamma K^{-\gamma-1}G + 2K^{-\gamma}G_S\frac{1-S}{K} + \frac{1}{1-\gamma}K^{1-\gamma}\Big[G_{SS}\frac{(1-S)^2}{K^2} - 2G_S\frac{1-S}{K^2}\Big], \\
J_{K_1K_2} &= -\gamma K^{-1-\gamma}G + K^{-\gamma}G_S\frac{1-2S}{K} + \frac{1}{1-\gamma}K^{1-\gamma}\Big[G_{SS}\frac{-(1-S)S}{K^2} + G_S\frac{2S-1}{K^2}\Big], \\
J_T &= \frac{1}{1-\gamma}K^{1-\gamma}G_T.
\end{aligned}
$$

Substituting the conjecture and its partial derivatives into the HJB equation leads to the following reduced-form HJB equation

$$
\delta G\log(G) = \sup_{i_1, i_2, f_1, f_2, r}\Big\{G_t + M_1 G + M_2 G_S + M_3 G_{SS} + M_4 G_T + M_5 G_{TT}\Big\} \tag{A.8}
$$

where $\mu_1 = \mu_1(i_1, r, T)$ and $\mu_2 = \mu_2(i_2, r, T, S)$ denote the drifts of the green and brown capital stocks, respectively. Furthermore, we introduce the three-dimensional volatility vectors

$$
\sigma_k(S) = \big((1-S)\sigma_1 + S\sigma_2\rho_{12},\, S\sigma_2\sqrt{1-\rho_{12}^2},\, 0\big)^\top, \tag{A.9}
$$

$$\sigma_s = \big(\sigma_2\rho_{12} - \sigma_1,\, \sigma_2\sqrt{1-\rho_{12}^2},\, 0\big)^\top. \tag{A.10}$$

The coefficients $M_\ell$ ($\ell = 1, \ldots, 5$) are given by

$$\begin{aligned}
M_1 &= (1-\gamma)\Big[\underbrace{(1-S)\mu_1 + S\mu_2}_{=\mu_k} - \frac{1}{2}\gamma[\underbrace{(1-S)^2\sigma_1^2 + S^2\sigma_2^2 + 2S(1-S)\sigma_1\sigma_2\rho_{12}}_{=\|\sigma_k\|^2}]\Big] \\
&\quad + \lambda_e\mathbb{E}[(1-\ell_e)^{1-\gamma} - 1] + \lambda_c(T)\mathbb{E}[(1-\ell_c)^{1-\gamma} - 1] + \delta(1-\gamma)\log(C/K) \\
M_2 &= S(1-S)\Big(\mu_2 - \mu_1 - \gamma\big[\underbrace{S\sigma_2^2 - (1-S)\sigma_1^2 + (1-2S)\sigma_1\sigma_2\rho_{12}}_{=\sigma_k^\top\sigma_s}\big]\Big) \\
M_3 &= \frac{1}{2}(1-S)^2S^2\big[\underbrace{\sigma_1^2 + \sigma_2^2 - 2\sigma_1\sigma_2\rho_{12}}_{=\|\sigma_s\|^2}\big] \\
M_4 &= \widehat{\beta} f_2 \\
M_5 &= \frac{1}{2}\sigma_T(T)^2
\end{aligned}$$

where $C/K$ is given in (A.7) and $\widehat{\beta} = \beta/K_2$. The separation thus holds if and only if $\widehat{\beta}$ is independent of $K_1$ and $K_2$, i.e., it has the representation $\widehat{\beta} = \widehat{\beta}(t, T, S)$. Calculating the first-order optimality conditions leads to the nonlinear system of equations (A.2)-(A.5) that determines the optimal controls. Finally, $q_1$ and $q_2$ satisfy

$$q_1 = \frac{C}{K}\frac{G - \frac{1}{1-\gamma}G_S S}{\delta G}, \qquad q_2 = \frac{C}{K}\frac{G + \frac{1}{1-\gamma}G_S(1-S)}{\delta G}.$$

This proves the proposition. □

# B Stochastic Discount Factor and Asset Prices

## B.1 Proof of Proposition 6.1

Duffie and Epstein (1992a) and Duffie and Skiadas (1994) show that the dynamics of the pricing kernel $H$ are given by (6.2) where the relevant partial derivatives of the aggregator are

$$f_c(C, J) = \frac{\delta(1-\gamma)GK^{1-\gamma}}{C}, \qquad f_J(C, J) = \delta(1-\gamma)\Big(\log\Big(\frac{C}{K}\Big) - \frac{1}{1-\gamma}\log G\Big) - \delta.$$

To calculate the dynamics of the SDF, we first compute

$$\frac{\mathrm{d}K^{-\gamma}}{K^{-\gamma}} = \Big( -\gamma\mu_k(i_1, i_2, r, T, S) + \frac{1}{2}\gamma(\gamma+1)\|\sigma_k\|^2\Big)\mathrm{d}t - \gamma\sigma_k^\top \mathrm{d}W + \sum_{i\in\{e,c\}} \big((1-\ell_i)^{-\gamma} - 1\big)\mathrm{d}N_i.$$

According to Ito's lemma, $G$ satisfies

$$\mathrm{d}G = G[\mu_g \mathrm{d}t + \sigma_g^\top \mathrm{d}W]$$

with

$$\begin{aligned}\mu_g &= \frac{1}{G}\Big(G_t + G_S S(1-S)\mu_s + G_T\beta f_2 + \frac{1}{2}G_{SS}S^2(1-S)^2\|\sigma_s\|^2 + \frac{1}{2}G_{TT}\sigma_T(T)^2\Big),\\ \sigma_g &= \frac{1}{G}\Big(G_S S(1-S)(-\sigma_1 + \sigma_2\rho_{12}),\ G_S S(1-S)\sigma_2\sqrt{1-\rho_{12}^2},\ G_T\sigma_T(T)\Big)^\top. \end{aligned} \tag{B.1}$$

Therefore, by Ito's product rule,

$$\begin{aligned}\frac{\mathrm{d}(GK^{-\gamma})}{GK^{-\gamma}} = &\Big( -\gamma\mu_k(i_1, i_2, r, T, S) + \frac{1}{2}\gamma(\gamma+1)\|\sigma_k\|^2\Big)\mathrm{d}t + \Big(\mu_g - \gamma\langle\sigma_k, \sigma_s\rangle\frac{G_S}{G}S(1-S)\Big)\mathrm{d}t\\ &+ (\sigma_g^\top - \gamma\sigma_k^\top)\mathrm{d}W + \sum_{i\in\{e,c\}} \big((1-\ell_i)^{-\gamma} - 1\big)\mathrm{d}N_i.\end{aligned}$$

Notice that according to (A.8), this expression can be simplified to

$$\begin{aligned}\frac{\mathrm{d}(GK^{-\gamma})}{GK^{-\gamma}} = &\Big[ -\mu_k + \gamma\|\sigma_k\|^2 - \sum_{i\in\{e,c\}} \lambda_i(T)\mathbb{E}[(1-\ell_i)^{1-\gamma} - 1] - \delta(1-\gamma)\log\chi + \delta\log G\Big]\mathrm{d}t\\ &+ (\sigma_g^\top - \gamma\sigma_k^\top)\mathrm{d}W + \sum_{i\in\{e,c\}} \big((1-\ell_i)^{-\gamma} - 1\big)\mathrm{d}N_i.\end{aligned}$$

The capital-consumption ratio $\chi = K/C^*$ has the following dynamics

$$\mathrm{d}\chi = \chi[\mu_\chi \mathrm{d}t + \sigma_\chi^\top \mathrm{d}W]$$

for auxiliary functions $\mu_\chi(t, S, T)$ and $\sigma_\chi(t, S, T)$ to be determined, see Appendix C.2. Then, the dynamics of $f_c$ are given by

$$\frac{\mathrm{d}f_c}{f_c} = \Big[ -\mu_k + \gamma\|\sigma_k\|^2 - \sum_{i\in\{e,c\}} \lambda_i(T)\mathbb{E}[(1-\ell_i)^{1-\gamma} - 1] - \delta(1-\gamma)\log\chi + \delta\log G + \mu_\chi\Big]\mathrm{d}t$$

$$+ \langle \sigma_g - \gamma\sigma_k, \sigma_\chi \rangle \mathrm{d}t + (\sigma_g^\top - \gamma\sigma_k^\top + \sigma_\chi^\top)\mathrm{d}W + \sum_{i\in\{e,c\}} \big((1-\ell_i)^{-\gamma} - 1\big)\mathrm{d}N_i$$

Consequently, the pricing kernel has the following dynamics

$$\begin{aligned}\frac{\mathrm{d}H}{H} &= \big[ -\delta - \mu_k + \gamma\|\sigma_k\|^2 + \sum_{i\in\{e,c\}} \lambda_i(T)\mathbb{E}[\ell_i(1-\ell_i)^{-\gamma}]\big]\mathrm{d}t + \big[\mu_\chi + \langle \sigma_g - \gamma\sigma_k, \sigma_\chi\rangle\big]\mathrm{d}t \\ &\quad + (\sigma_g^\top - \gamma\sigma_k^\top + \sigma_\chi^\top)\mathrm{d}W + \sum_{i\in\{e,c\}} \big((1-\ell_i)^{-\gamma} - 1\big)\mathrm{d}N_i - \lambda(T)\mathbb{E}[(1-\ell)^{-\gamma} - 1]\big]\mathrm{d}t.\end{aligned} \tag{B.2}$$

An application of Itô's lemma shows that the drift rate and the volatility vector of optimal consumption is given by

$$\mu_c(t,S,T) = \mu_k(S) - \mu_\chi(t,S,T) + \|\sigma_\chi(t,S,T)\|^2 - \langle \sigma_\chi(t,S,T), \sigma_k(S)\rangle, \tag{B.3}$$

$$\sigma_c(t,S,T) = \sigma_k(S) - \sigma_\chi(t,S,T). \tag{B.4}$$

Substituting (B.3) and (B.4) into (B.2) and some algebra finishes the proof. □

## B.2 Dividend Dynamics

Dividends of asset $n$ are given by

$$D_n = Y_n - I_n - b_n F_n = \big[A_n f_n^{\eta_n}\Lambda_n(T) - i_n - b_n f_n\big]K_n$$

for $n \in \{1,2\}$. It follows from Proposition A.1 that the term in the square brackets only depends on $t$, $S$, and $T$, but not on $K_1$ or $K_2$. Consequently, we can write the dividends as

$$D_n = \delta_n(t,S,T)K_n \tag{B.5}$$

for functions $\delta_n$ that can be determined numerically using the approach described in Appendix C.1. Notice that in equilibrium, the state variables $S$ and $T$ are continuous processes. In turn, the $\delta_n$ are continuous functions and follow the dynamics

$$\mathrm{d}\delta_n = \delta_n(\mu_{\delta_n}\mathrm{d}t + \sigma_{\delta_n}^\top \mathrm{d}W)$$

where subscripts of $\delta_n$ denote partial derivatives and where drift and volatility are given by

$$\mu_{\delta_n} = \frac{1}{\delta_n}\big[\delta_{n,t} + \delta_{n,S}S(1-S)\mu_S + \delta_{n,T}\mu_T + \frac{1}{2}\delta_{n,TT}\|\sigma_T\|^2 + \frac{1}{2}\delta_{n,SS}S^2(1-S)^2\|\sigma_S\|^2\big],$$
$$\sigma_{\delta_n} = \frac{1}{\delta_n}\big[\delta_{n,T}\sigma_T + \delta_{n,S}S(1-S)\sigma_S\big].$$

An application of Itô's product rule to (B.5) yields the dividend dynamics

$$\mathrm{d}D_i = D_{n-}\Big[\mu_{D_n}\mathrm{d}t + \sigma_{D_n}^\top \mathrm{d}W - \sum_{i\in\{c,e\}} \ell_i \mathrm{d}N_i\Big] \tag{B.6}$$

with

$$\mu_{D_n} = \mu_{K_n} + \mu_{\delta_n} + \sigma_{\delta_n}^\top \sigma_{K_n} \qquad \text{and} \qquad \sigma_{D_n} = \sigma_{K_n} + \sigma_{\delta_n}.$$

In a second step, we determine the dynamics of discounted dividends, $\widehat{D}_i = HD_i$. Another application of Itô's product rule implies

$$\begin{aligned}\mathrm{d}\widehat{D}_n &= D_{n-}\mathrm{d}H + H_-\mathrm{d}D_n + \mathrm{d}\langle D_n^c, H^c\rangle + \Delta D_n \Delta H \\ &= \widehat{D}_{n-}\Big[\mu_{\widehat{D}_n}(S,T)\mathrm{d}t + \sigma_{\widehat{D}_n}(T,S)^\top \mathrm{d}W + \sum_{i\in\{c,e\}} \big((1-\ell_i)^{1-\gamma} - 1\big)\mathrm{d}N_i\Big]\end{aligned}$$

with

$$\mu_{\widehat{D}_n} = \mu_H + \mu_{D_n} + \Theta_H^\top \sigma_{D_n} \qquad \text{and} \qquad \sigma_{\widehat{D}_n} = \Theta_H + \sigma_{D_n}.$$

## B.3 Price-dividend Ratios of Dividend Claims

Let $\omega_n = \log\left(\frac{P_n}{D_n}\right)$ denote the log price-dividend ratio of asset $n$. Due to the representation (B.5) of the dividends, the dynamics of $K_n$, and the pricing equation (6.4), the price is linear in $K_n$ and thus the price-dividend ratio is independent of $K_n$. Therefore, it is a continuous process with dynamics

$$\begin{aligned}\mathrm{d}\omega_n &= \omega_{n,t}\mathrm{d}t + \omega_{n,S}\mathrm{d}S + \omega_{n,T}\mathrm{d}T + \frac{1}{2}\omega_{n,TT}\|\sigma_T\|^2\mathrm{d}t + \frac{1}{2}\omega_{n,SS}S^2(1-S)^2\|\sigma_S\|^2\mathrm{d}t \\ &= \omega_n(\mu_{\omega_n}\mathrm{d}t + \sigma_{\omega_n}^\top \mathrm{d}W)\end{aligned}$$

where the drift and the volatility vector are given by

$$\mu_{\omega_n} = \frac{1}{\omega_i}\big[\omega_{n,t} + \omega_{n,S}S(1-S)\mu_S + \omega_{n,T}\mu_T + \frac{1}{2}\omega_{n,TT}\|\sigma_T\|^2 + \frac{1}{2}\omega_{n,SS}S^2(1-S)^2\|\sigma_S\|^2\big]$$
$$\sigma_{\omega_n} = \frac{1}{\omega_i}\big[\omega_{n,T}\sigma_T + \omega_{n,S}S(1-S)\sigma_S\big].$$

In particular, the price-dividend ratio $\mathrm{e}^{\omega_n} = \frac{P_n}{D_n}$ satisfies the following dynamics

$$\mathrm{d}(\mathrm{e}^{\omega_n}) = \mathrm{e}^{\omega_n}\omega_n\Big[\big(\mu_{\omega_n} + \frac{1}{2}\|\sigma_{\omega_n}\|^2\big)\mathrm{d}t + \sigma_{\omega_n}^\top \mathrm{d}W\Big].$$

We rewrite the discounted asset price $HP_n$ as $F_n(\widehat{D}_n, \omega_n) = \widehat{D}_n\mathrm{e}^{\omega_n}$. An application of the Feynman-Kač Theorem yields

$$\mathcal{L}F_n + \mathrm{e}^{-\omega_n}F_n = 0, \tag{B.7}$$

where $\mathcal{L}F_n$ denotes the infinitesimal generator. It follows from Itô's lemma that

$$\frac{\mathrm{d}F_n}{F_{n-}} = \big(\mu_H + \mu_{D_n} + \mu_{\omega_n} + \frac{1}{2}\|\sigma_{\omega_n}\|^2 + \sigma_{\omega_n}^\top\Theta_H + \sigma_{\omega_n}^\top\sigma_{D_n} + \Theta_H^\top\sigma_{D_n}\big)\mathrm{d}t + (\sigma_{\omega_n} + \sigma_{D_n} + \Theta_H)^\top\mathrm{d}W$$
$$+ \sum_{i\in\{c,e\}}\big((1-\ell_i)^{1-\gamma} - 1\big)\mathrm{d}N_i\big].$$

The no-arbitrage condition implies

$$\frac{\mathrm{d}F_n}{F_{n-}} = \mu_H + \mu_{D_n} + \mu_{\omega_n} + \frac{1}{2}\|\sigma_{\omega_n}\|^2 + \sigma_{\omega_n}^\top\Theta_H + \sigma_{\omega_n}^\top\sigma_{D_n} + \Theta_H^\top\sigma_{D_n} + \sum_{i\in\{c,e\}}\lambda_i(T)\mathbb{E}\big[(1-\ell_i)^{1-\gamma} - 1\big]. \tag{B.8}$$

Substituting (B.8) into (B.7) yields

$$0 = \mu_H + \mu_{D_n} + \mu_{\omega_n} + \frac{1}{2}\|\sigma_{\omega_n}\|^2 + \sigma_{\omega_n}^\top\Theta_H + \sigma_{\omega_n}^\top\sigma_{D_n} + \Theta_H^\top\sigma_{D_n} + \sum_{i\in\{c,e\}}\lambda_i(T)\mathbb{E}\big[(1-\ell_i)^{1-\gamma} - 1\big] + \mathrm{e}^{-\omega_n}.$$

Consequently, we end up with the following partial differential equation for $\omega_n$:

$$0 = \mu_H + \mu_{D_n} + \Theta_H^\top\sigma_{D_n} + \mathrm{e}^{-\omega_n} + \omega_{n,t} + \omega_{n,S}S(1-S)\mu_S + \omega_{n,T}\mu_T + \frac{1}{2}(\omega_{n,TT} + \omega_{n,T}^2)\|\sigma_T\|^2$$
$$+ \frac{1}{2}(\omega_{n,SS} + \omega_{n,S}^2)S^2(1-S)^2\|\sigma_S\|^2 + \big(\omega_{n,T}\sigma_T + \omega_{n,S}S(1-S)\sigma_S\big)^\top\Theta_H$$

$$+ \left(\omega_{n,T}\sigma_T + \omega_{n,S}S(1-S)\sigma_S\right)^\top \sigma_{D_n} + \sum_{i\in\{c,e\}} \lambda_i(T)\mathbb{E}\left[(1-\ell_i)^{1-\gamma} - 1\right]$$

Notice that this PDE is nonlinear as it involves squared partial derivatives of $\omega_n$. To simplify the numerical solution approach, we transform this PDE into a linear, parabolic PDE that can be solved with a similar approach as described in Appendix C.1. We substitute $\Omega_n = \mathrm{e}^{\omega_n}$ and end up with

$$\begin{aligned} 0 = 1 &+ \Omega_n\Big(\mu_H + \mu_{D_n} + \Theta_H^\top\sigma_{D_n} + \sum_{i\in\{c,e\}} \lambda_i(T)\mathbb{E}\left[(1-\ell_i)^{1-\gamma} - 1\right]\Big) + \Omega_{n,t} + \Omega_{n,S}S(1-S)\mu_S \\ &+ \Omega_{n,T} + \mu_T\frac{1}{2}\Omega_{n,TT}\|\sigma_T\|^2 + \frac{1}{2}\Omega_{n,SS}S^2(1-S)^2\|\sigma_S\|^2 \\ &+ (\Omega_{n,T}\sigma_T + \Omega_{n,S}S(1-S)\sigma_S)^\top(\Theta_H + \sigma_{D_n}) \end{aligned} \tag{B.9}$$

## B.4 Risk Premia

The dynamics of the asset price $P_n = \mathrm{e}^{\omega_n}D_n$ follow via Itô's lemma. We obtain the following asset price dynamics

$$\frac{\mathrm{d}P_n}{P_n} = \mu_{P_n}\mathrm{d}t + \sigma_{P_n}^\top \mathrm{d}W - \sum_{i\in\{c,e\}} \ell_i \mathrm{d}N_i + \sum_{i\in\{c,e\}} \lambda_i(T)\mathbb{E}[\ell_i]\mathrm{d}t$$

where the expected stock return and the volatility vector are given by

$$\mu_{P_n} = \mu_{\omega_n} + \mu_{K_n} + \mu_{\delta_n} + \sigma_{\delta_n}^\top\sigma_{K_n} + \sigma_{K_n}^\top\sigma_{\omega^i} + \sigma_{\delta_n}^\top\sigma_{\omega^i} + \frac{1}{2}\|\sigma_{\omega_n}\|^2 - \sum_{i\in\{c,e\}} \lambda_i(T)\mathbb{E}[\ell_i]$$

$$\sigma_{P_n} = \sigma_{\omega_n} + \sigma_{K_n} + \sigma_{\delta_n}$$

Now, the risk premium of asset $n$ can be computed as the sum of its expected stock return, $\mu_{P_n}$, and its dividend yield, $\mathrm{e}^{-\omega_n}$, minus the risk-free interest rate, $r^f$, i.e.,

$$\mathrm{rp}_n = \mu_{P_n} + \mathrm{e}^{-\omega_n} - r^f.$$

# C Numerical Solution Approach

## C.1 Indirect Utility Function and Optimal Controls

**Basic idea** We face a problem with an infinite time horizon. Since the boundary conditions on $G$ are unknown, we transform the problem into a similar one with a finite time horizon denoted by $t_{\max}$. In our implementation, we consider a model with a finite time horizon and set $G(t_{\max}, T, S) = 1$, which can be interpreted as that the economy consumes the whole capital stock at $t_{\max}$. Starting with this terminal condition, we work backwards through the time grid until the differences between the indirect utility function in $t+1$ and $t$ become negligibly small and the solution converges to that of an infinite time horizon.

**Definition of the grid** We use a grid-based solution approach to solve the non-linear PDE. We discretize the $(t, T, S)$-space using an equally-spaced lattice. Its grid points are defined by

$$\big\{(t_n, T_i, S_j) \mid n = 0, \cdots, N_t,\, i = 0, \cdots, N_T,\, j = 0, \cdots, N_S\big\},$$

where $t_n = n\Delta_t$, $T_i = i\Delta_T$, and $S_j = j\Delta_S$ for some fixed grid size parameters $\Delta_t$, $\Delta_T$, and $\Delta_S$ that denote the distances between two grid points. The numerical results are based on a choice of $N_T = 1000$, $N_S = 500$ and 1 time step per year. Our results hardly change if we use a finer grid or more time steps per year. In the sequel, $G_{n,i,j}$ denotes the approximated indirect utility function at the grid point $(t_n, T_i, S_j)$ and $\pi_{n,i,j}$ refers to the corresponding set of optimal controls. We apply an implicit finite-difference scheme.

**Finite differences approach** In this paragraph, we describe the numerical solution approach in more detail. We adapt the numerical solution approach used by Munk and Sørensen (2010). The numerical procedure works as follows. At any point in time, we make a conjecture for the optimal abatement policy $\pi^*_{n,i,j}$. A good guess is the value at the previous grid point since the abatement strategy varies only slightly over a small time interval, i.e., we set $\pi_{n-1,i,j} = \pi^*_{n,i,j}$. Substituting this guess into the HJB equation yields a semi-linear PDE:

$$0 = -\delta \log(G)G + M_1 G + M_2 G_T + M_3 G_{TT} + M_4 G_S + M_5 G_{SS}$$

with state-dependent coefficients $M_i = M_i(t, T, S)$ as stated in Appendix A. Due to the implicit approach, we approximate the time derivative by forward finite differences. In the approximation, we use the so-called 'up-wind' scheme that stabilizes the finite differences approach. Therefore, the relevant finite differences at the grid point $(n, i, j)$ are given by

$$\begin{aligned}
&\mathrm{D}_T^+ G_{n,i,j} = \frac{G_{n,i+1,j} - G_{n,i,j}}{\Delta_T}, \qquad \mathrm{D}_T^- G_{n,i,j} = \frac{G_{n,i,j} - G_{n,i-1,j}}{\Delta_T}, \\
&\mathrm{D}_S^+ G_{n,i,j} = \frac{G_{n,i,j+1} - G_{n,i,j}}{\Delta_S}, \qquad \mathrm{D}_S^- G_{n,i,j} = \frac{G_{n,i,j} - G_{n,i,j-1}}{\Delta_S}, \\
&\mathrm{D}_{TT}^2 G_{n,i,j} = \frac{G_{n,i+1,j} - 2G_{n,i,j} + G_{n,i-1,j}}{\Delta_T^2}, \qquad \mathrm{D}_{SS}^2 G_{n,i,j} = \frac{G_{n,i,j+1} - 2G_{n,i,j} + G_{n,i,j-1}}{\Delta_S^2} \\
&\mathrm{D}_t^+ G_{n,i,j} = \frac{G_{n+1,i,j} - G_{n,i,j}}{\Delta_t}.
\end{aligned}$$

Substituting these expressions into the PDE above yields the following semi-linear equation for the grid point $(t_n, m_i, \tau_j)$

$$\begin{aligned}
G_{n+1,i,j}\frac{1}{\Delta_t} = G_{n,i,j}\Big[ &- M_1 + \frac{1}{\Delta_t} + \mathrm{abs}\Big(\frac{M_2}{\Delta_T}\Big) + \mathrm{abs}\Big(\frac{M_4}{\Delta_S}\Big) + 2\frac{M_3}{\Delta_T^2} + 2\frac{M_5}{\Delta_S^2}\Big] \\
&+ G_{n,i-1,j}\Big[\frac{M_2^-}{\Delta_T} - \frac{M_3}{\Delta_T^2}\Big] + G_{n,i+1,j}\Big[ - \frac{M_2^+}{\Delta_T} - \frac{M_3}{\Delta_T^2}\Big] \\
&+ G_{n,i,j-1}\Big[\frac{M_4^-}{\Delta_S} - \frac{M_5}{\Delta_S^2}\Big] + G_{n,i,j+1}\Big[ - \frac{M_4^+}{\Delta_S} - \frac{M_5}{\Delta_S^2}\Big] \\
&+ \delta G_{n,i,j}\log(G_{n,i,j})
\end{aligned}$$

Therefore, for a fixed point in time each grid point is determined by a non-linear equation. This results in a non-linear system of $(N_S + 1)(N_T + 1)$ equations that can be solved for the vector

$$G_n = (G_{n,1,1}, \cdots, G_{n,1,N_S}, G_{n,2,1}, \cdots, G_{n,2,N_S}, \cdots, G_{n,N_T,1}, \cdots, G_{n,N_T,N_S}).$$

Using this solution we update our conjecture for the optimal controls at the current point in the time dimension. We apply the first-order conditions and finite difference approximations of the corresponding derivatives. In the interior of the grid, we use centered finite differences. At the boundaries, we apply forward or backward differences.

### C.2 Stochastic Discount Factor and Risk Premia

The dynamics of the SDF and the asset prices involve some yet unknown variables. For instance, the risk-free rate (6.3) or the dividend dynamics (B.6) involve the unknown drift and volatility vector of the capital-consumption ratio or the dividend-capital ratio, respectively. These variables depend on the reduced indirect utility function $G$ in (A.1) and its partial derivatives in a highly nonlinear manner. We thus calculate these variables numerically using finite differences. An application of Itôs lemma to $\chi = \chi(t, S, T)$ implies

$$\mathrm{d}\chi = \chi_t \mathrm{d}t + \chi_S \mathrm{d}S + \chi_T \mathrm{d}T + \frac{1}{2}\chi_{TT}\|\sigma_T\|^2 \mathrm{d}t + \frac{1}{2}\chi_{SS}\|\sigma_S\|^2 \mathrm{d}t$$

where

$$\mu_\chi(t, S, T) = \frac{1}{\chi}\big[\chi_t + \chi_S S(1-S)\mu_S + \chi_T \mu_T + \frac{1}{2}\chi_{TT}\|\sigma_T\|^2 + \frac{1}{2}\chi_{SS}S^2(1-S)^2\|\sigma_S\|^2\big], \quad \text{(C.1)}$$

$$\sigma_\chi(t, S, T) = \frac{1}{\chi}\big[\chi_S S(1-S)\sigma_S + \chi_T \sigma_T\big] \quad \text{(C.2)}$$

Since $\chi = \big((1-S)[A_1 f_1^{\eta_1}\Lambda_1(T) - i_1 - b_1 f_1] + S[A_2 f_2^{\eta_2}\Lambda_2(T) - i_2 - b_2 f_2]\big)^{-1}$ and the optimal controls have already be calculated, we can use finite differences again to determine $\chi$ and its partial derivatives. Then, we substitute them into (C.1) and (C.2) to obtain the relavant drift and volatility vector.

## D Details on the Calibration

To calibrate the relevant parameters, we follow Pindyck and Wang (2013). Their model only involves a single capital stock and abstracts from climate change, but it is nested by our two-sector model. The model is well-suited to explain *historical* asset returns, since dirty capital has dominated the world economy in the past, but the influence of climate change on asset markets was almost negligible. In the long run, there might be a transition from dirty to green capital. Yet, the current share of green capital is only about 6% indicating that the transition

to green energy has been very modest so far.[24] We consider the special case of our model with only one capital stock evolving as

$$\mathrm{d}K = \Big(I - \frac{1}{2}\phi\frac{I^2}{K} - \delta_k K\Big)\mathrm{d}t + K\sigma\mathrm{d}W_1 - K\ell_e\mathrm{d}N_e.$$

and output given by $Y = AK^{1-\eta}F^{\eta} = I + C + bF$. In the optimum, the model collapses to a simple $AK$-technology with linear production function $Y = A^*K$ where productivity is

$$A^* = A\Big(\frac{b}{\eta A}\Big)^{\frac{\eta}{\eta-1}}.$$

The one-sector model is close to that of Pindyck and Wang (2013), but involves energy input $F$ which does not cause climate change. We choose the parameters to generate a real expected growth rate of consumption of $\overline{\mu}_c = 2\%$, an average consumption rate of $\frac{C}{A^*K} = 75\%$ of GDP, a risk-free interest rate starting at $r^f = 0.8\%$, an average risk premium of $\mathrm{rp} = 6.3\%$, and Tobin'Q's of $q = 1.5$. The following equations constitute a non-linear system that relates $\delta$, $\gamma$, $A^*$, $\phi$, and $\delta_K$ to these quantities

$$\frac{C}{A^*K} = \frac{\phi - A^* + \sqrt{(\phi - A^*)^2 + 4\phi\delta}}{2\phi} \tag{D.1}$$

$$\overline{\mu}_c = -\delta_k K + A\Big(1 - \frac{C}{A^*K} - \eta\Big) - \frac{1}{2}\phi A^2\Big(1 - \frac{C}{A^*K} - \eta\Big)^2 - \frac{\lambda_e}{\alpha_e + 1} \tag{D.2}$$

$$r^f = \delta + \overline{\mu}_c - \frac{1}{2}\sigma_c^2 - \lambda_e\frac{(1-\gamma)(\alpha_e - \gamma) + \gamma(\alpha_e - \gamma + 1)}{(\alpha_e - \gamma)(\alpha_e - \gamma + 1)} + \frac{\lambda_e}{\alpha_e + 1} \tag{D.3}$$

$$\mathrm{ep} = \gamma\sigma_c^2 + \lambda_e\gamma\Big[\frac{1}{\alpha_e - \gamma} - \frac{\alpha_e}{(\alpha_e + 1)(\alpha_e - \gamma + 1)}\Big] \tag{D.4}$$

$$q = \frac{1}{1 - \phi i} \tag{D.5}$$

For the derivation of these equations and for further details, we refer to Pindyck and Wang (2013).

[24] See the website of the UNFCCC. https://unfccc.int/news/green-economy-overtaking-fossil-fuel-industry-ftse-russel-report

| | | |
|---|---|---|
| | **Preferences** | |
| $\delta$ | time-preference rate | 0.05 |
| $\gamma$ | relative risk aversion | 5.288 |
| $\psi$ | elasticity of intertemporal substitution | 1 |
| | **Economic Model** | |
| $Y_0$ | initial GDP (trillion US \$) | 75.8 |
| $S_0$ | initial share of dirty capital | 0.94 |
| $A_1$ | green productivity | 0.851 |
| $A_2$ | brown productivity | 0.828 |
| $b_1$ | fossil fuel costs (\$ per tC) | 540 |
| $b_2$ | green energy costs (\$ per etC) | 810 |
| $\eta_n$ | energy share in production | 0.066 |
| $\phi_n$ | investment adjustment cost parameter | 18.12 |
| $\sigma_n$ | annual capital volatility | 0.02 |
| $\alpha_e$ | macroeconomic jump size parameter | 8 |
| $\lambda_e$ | macroeconomic disaster intensity parameter | 0.088 |
| $\kappa$ | capital reallocation cost parameter | 1 |
| $\rho_{12}$ | instantaneous correlation | 0 |
| | **Climate Model** | |
| $T_0$ | initial temperature (°C) | 1 |
| $\sigma_T$ | temperature diffusion coefficient | 0.015 |
| $\vartheta$ | TCRE (°C/TtC) | 1.8 |
| $p_0$ | emission intensity parameter | 11.03 |
| $p_1$ | emission intensity parameter | 0.1979 |
| $p_2$ | emission intensity parameter | $-8.554 \times 10^{-4}$ |

**Table 1: Benchmark Calibration.** This table summarizes the parameters of the benchmark calibration with 2015 as base year. It is described in Section 4.

| Specification | Calibration |
|---|---|
| Level Impact (L–I) | $\theta_i = 0.00236$ |
| Disaster Impact (D–I) | $\lambda_c(T) = 0.003 + 0.096T$, $\alpha_c = 65.67$ |
| Growth Rate Impact (G–I) | $\xi_i = 0.00144$ |

**Table 2: Three Types of Specifications for Global Warming Damages.** The table summarizes the different damage specifications that are studied in this paper.

| Impact | Benchmark (—) | Double Impact (—) | Triple Impact (—) |
|---|---|---|---|
| Level | $\theta_i = 0.00236$ | $\theta_i = 0.00472$ | $\theta_i = 0.00708$ |
| Disaster | $\lambda_c(T) = 0.003 + 0.096T$ | $\lambda_c(T) = 0.003 + 0.192T$ | $\lambda_c(T) = 0.003 + 0.288$ |
| Growth Rate | $\xi_i = 0.00144$ | $\xi_i = 0.00288$ | $\xi_i = 0.00432$ |

**Table 3: Different Intensities for the Specifications of Global Warming Damages.** The table summarizes the different damage specifications that are used in Figure 3.

| | $r_f$ | $\mu_c$ | $-\gamma\|\sigma_c\|^2$ | $-\langle\sigma_g + (\gamma-1)\sigma_c, \sigma_k - \sigma_c\rangle$ |
|---|---|---|---|---|
| $T = 1°\text{C}$ | 0.82% | 2.92% | –0.11% | 0.00% |
| $T = 2°\text{C}$ | 0.77% | 2.87% | –0.11% | 0.00% |
| $T = 3°\text{C}$ | 0.71% | 2.81% | –0.11% | –0.00% |
| $T = 4°\text{C}$ | 0.64% | 2.74% | –0.11% | –0.01% |
| $T = 5°\text{C}$ | 0.55% | 2.67% | –0.11% | –0.02% |
| $S = 0.05$ | 0.75% | 2.94% | –0.19% | –0.00% |
| $S = 0.25$ | 0.76% | 2.89% | –0.13% | –0.00% |
| $S = 0.50$ | 0.73% | 2.83% | –0.11% | –0.00% |
| $S = 0.75$ | 0.66% | 2.78% | –0.13% | 0.00% |
| $S = 0.95$ | 0.53% | 2.71% | –0.19% | –0.00% |

**Table 4: Risk-free Rate Decomposition for the Year 2100.** The table shows the state-dependent terms in the decomposition of the risk-free rate (6.3). It provides sensitivity analysis for different values of temperature and the share of dirty capital around their median values in 2100 ($S = 0.53$, $T = 2.8$). The constant terms in (6.3) are the time preference rate $\delta = 0.05$, the contribution of economic disasters $\lambda_e \mathbb{E}_t[\ell_e(1-\ell_e)^{-\gamma}] = 0.0699$, and the contribution of climate-related disasters $\lambda_c \mathbb{E}_t[\ell_c(1-\ell_c)^{-\gamma}] = 0$.

| | Green Asset | | | Dirty Asset | | | Risk-free rate |
|---|---|---|---|---|---|---|---|
| | $\text{rp}_1$ | $\mu_{P_1}$ | $\Omega_1^{-1}$ | $\text{rp}_2$ | $\mu_{P_2}$ | $\Omega_2^{-1}$ | $r_f$ |
| $T = 1°\text{C}$ | 6.45% | 2.82% | 4.38% | 6.30% | 1.70% | 5.35% | 0.82% |
| $T = 2°\text{C}$ | 6.47% | 2.94% | 4.19% | 6.28% | 1.44% | 5.50% | 0.77% |
| $T = 3°\text{C}$ | 6.48% | 3.02% | 4.02% | 6.26% | 1.18% | 5.64% | 0.71% |
| $T = 4°\text{C}$ | 6.50% | 3.08% | 3.88% | 6.25% | 0.93% | 5.78% | 0.64% |
| $T = 5°\text{C}$ | 6.51% | 3.10% | 3.77% | 6.24% | 0.69% | 5.90% | 0.55% |
| $S = 0.05$ | 6.22% | 1.99% | 4.98% | 6.03% | 2.05% | 4.73% | 0.75% |
| $S = 0.25$ | 6.21% | 2.02% | 4.89% | 6.09% | 2.01% | 4.77% | 0.76% |
| $S = 0.50$ | 6.46% | 2.89% | 4.17% | 6.29% | 1.34% | 5.55% | 0.73% |
| $S = 0.75$ | 6.63% | 4.11% | 2.98% | 6.21% | 0.91% | 5.76% | 0.66% |
| $S = 0.95$ | 6.80% | 5.82% | 1.26% | 6.30% | 1.32% | 5.25% | 0.53% |

**Table 5: Risk Premium Decomposition for the Year 2100.** The table shows the decomposition of the risk-premium $\text{rp}_i$ into its components dividend yield $\Omega_i^{-1}$, stock growth rate $\mu_{P_i}$, and risk-free rate $r_f$. It provides sensitivity analysis for different values of the share of dirty capital and temperature around their median values in 2100 ($S = 0.53$, $T = 2.8$). We use the benchmark calibration from Section 4.

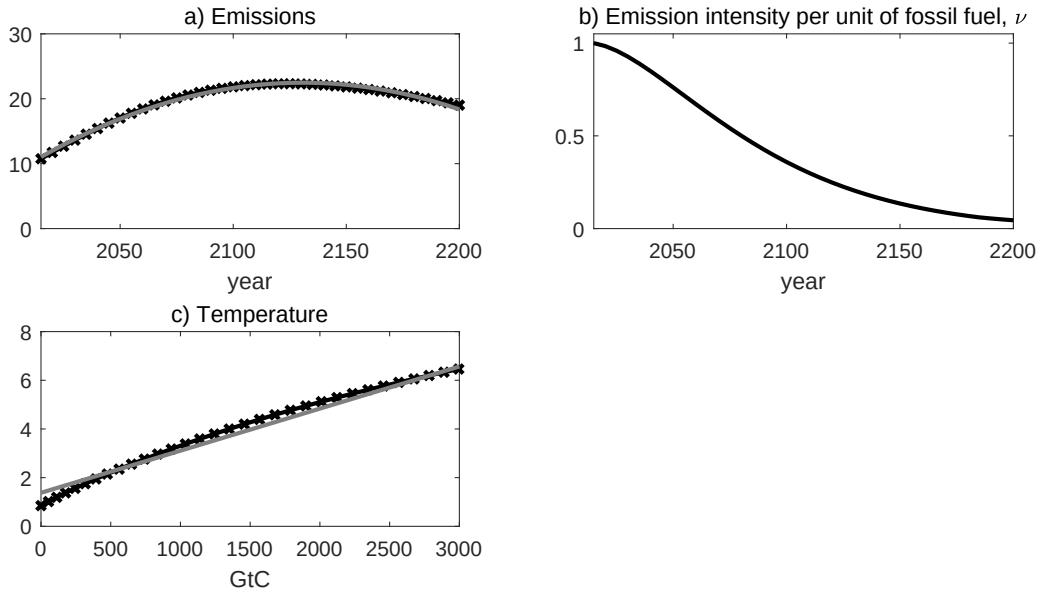


**Figure 1: Calibration of the Climate System.** Panel (a) shows carbon dioxide emissions in the BAU-scenario in DICE (black crosses). The gray line depicts the BAU evolution in our model. The emission intensity per unit of fossil fuel is plotted in Panel (b). Panel (c) shows the relation of cumulative emissions and temperature increase in DICE. The gray line shows a linear least-squares fit to this data. The slope of this straight line gives a Transient Climate Response to Cumulative Emissions (TCRE) of 1.8°C/TtC.

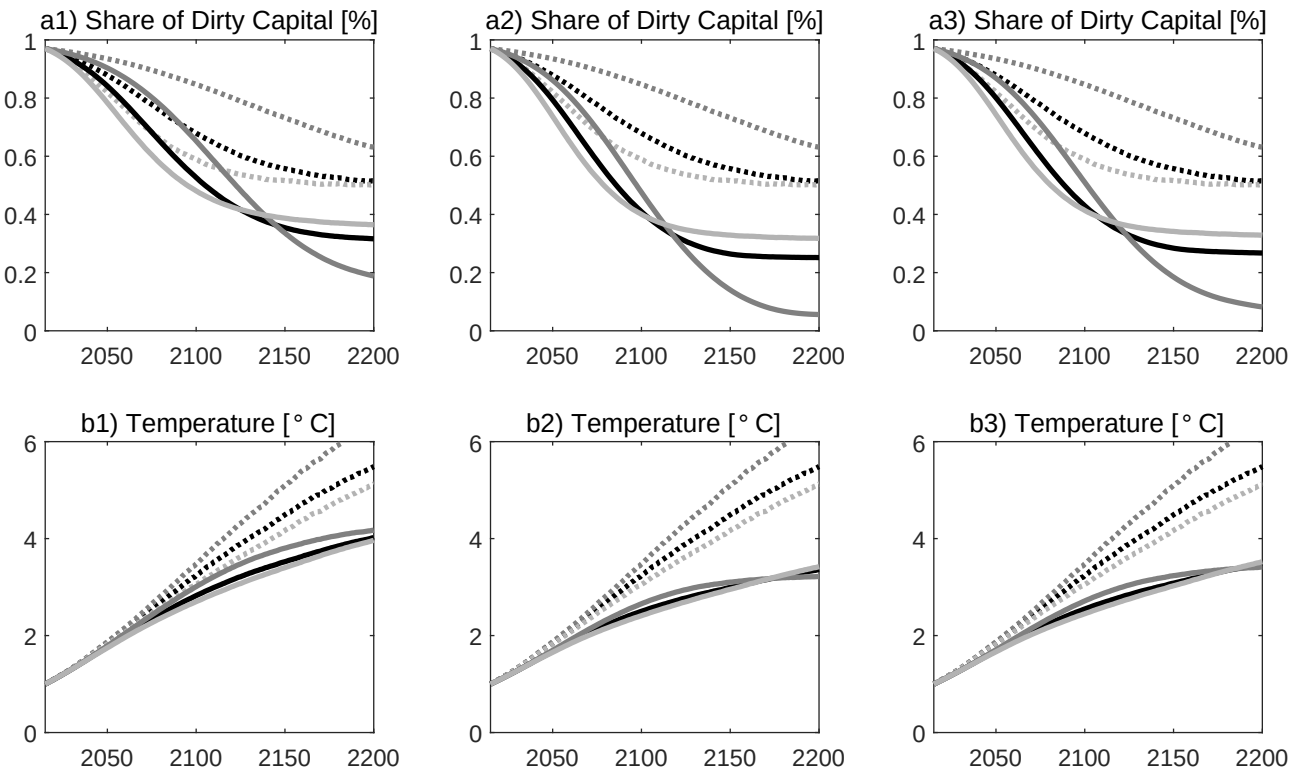


**Figure 2: Varying the Correlation Coefficient between the Two Sectors.** Solid lines depict the optimal evolution of the share of dirty capital and global average temperature for the three damage specifications level impact (1st column), disaster impact (2nd column), and growth rate impact (3rd column) until the year 2200. Black lines (⋯⋯,——) show results for the benchmark case where the correlation between the Brownian shocks affecting the green and dirty sector is $\rho_{12} = 0$. Gray lines (⋯⋯, ——) show results with $\rho_{12} = 0.5$. Light lines (⋯⋯, ——) depict the results with $\rho_{12} = -0.5$. Dotted lines show the corresponding results for hypothetical scenarios without damages from climate change. The main insight from this figure is that initially it is important to drive down the carbon-intensive part of the economy for both diversification and abatement reasons, but once the share of dirty capital has fallen below its optimal share in the absence of climate damages the carbon-intensive part of the economy is driven down purely for abatement reasons at the expense of the diversification objective.

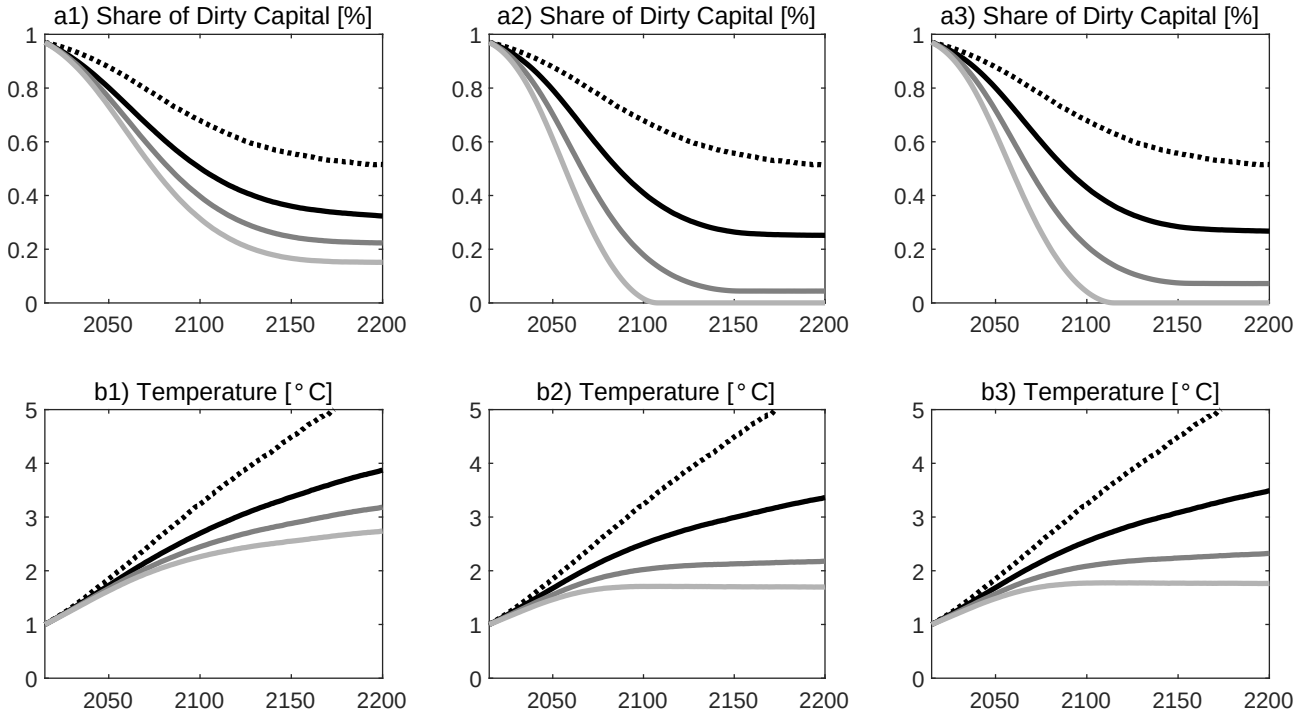


**Figure 3: Increasing Intensities of Global Warming Damages.** The figure depicts the simulation of the share of dirty capital and global average temperature for the three damage specifications level impact (1st column), disaster impact (2nd column) and growth rate impact (3rd column) until the year 2200. The black dotted lines (⋯⋯) show the results for a hypothetical scenario without damages from climate change. The black solid lines (——) show the results for the damage parameters as calibrated in Section 4. The gray lines (——) show results with damage parameters that are twice as high as in the benchmark calibration. The light lines (——) show results with damage parameters that are three times higher than those from the benchmark calibration. The main insight from this figure is that with higher intensities of damages than our benchmark damages, the abatement motives becomes relatively more important than the diversification motive and leads to a lower or even a zero dirty capital stock in the long run.

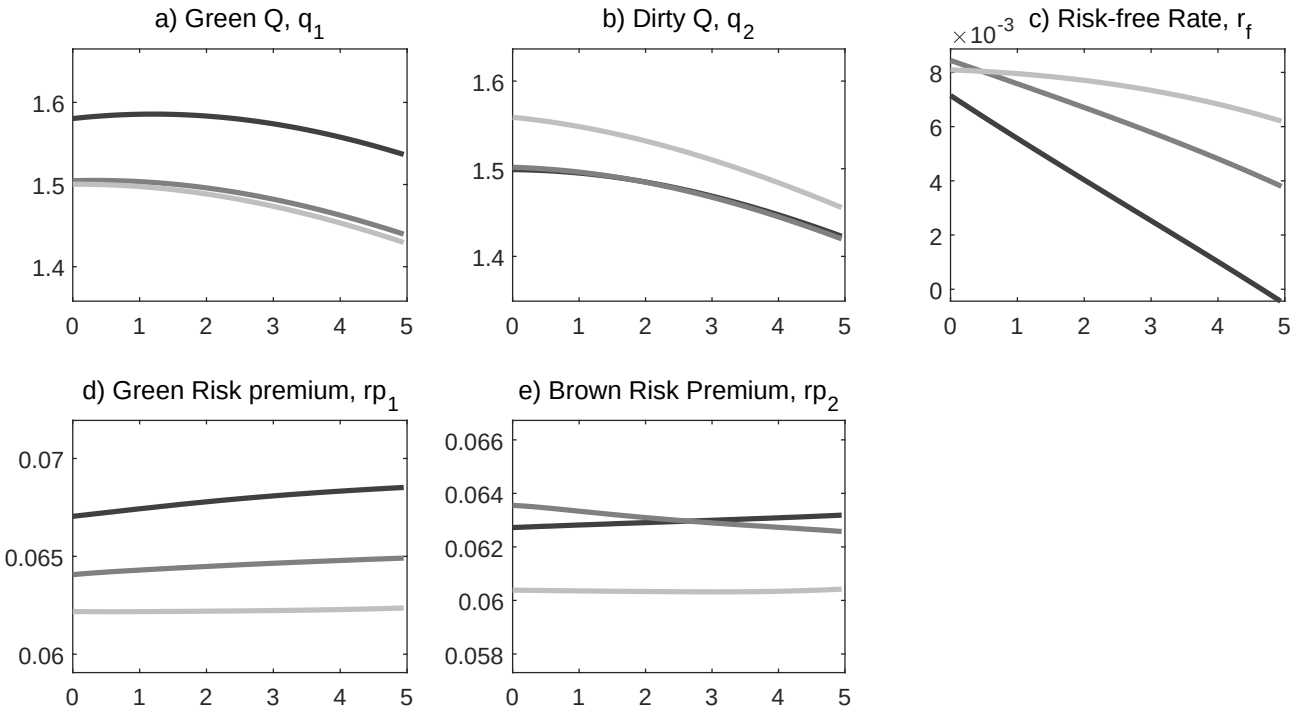


**Figure 4: Asset Pricing versus Temperature and the Share of Dirty Capital.** On the horizontal axis is temperature in the range from 0°C to 5°C. The lines represent various levels of the capital share: dark lines (——) depict $S = 0.95$, gray lines (——) refer to $S = 0.5$, and light (——) lines to $S = 0.05$. a) plots Tobin's Q of the green asset, b) shows Tobin's Q of the dirty capital stock, c) depicts the equilibrium risk-free rate, d) shows the risk premium of the green asset, e) depicts the risk premium of the dirty asset. The option to convert dirty capital into green capital generates interesting qualitative effects but the quantitative implications are modereate.

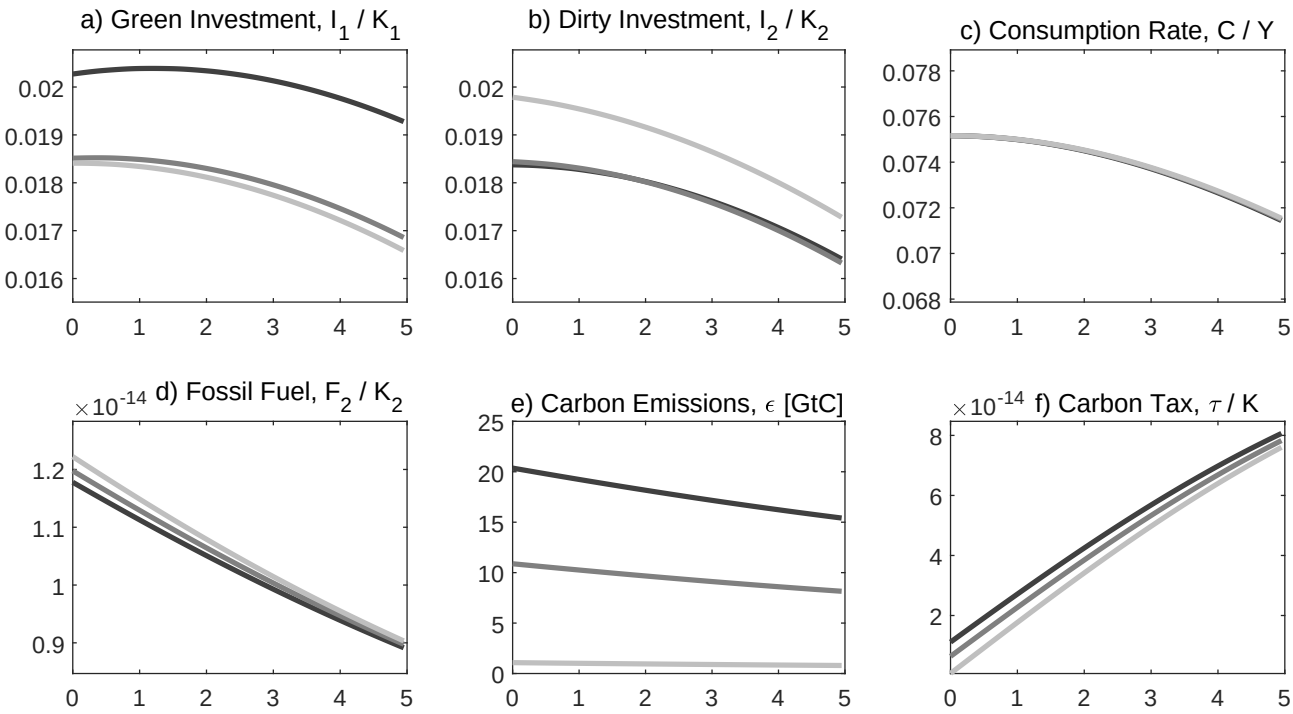


**Figure 5: Policy Function with only Level Impact (L-I) Global Warming Damages.** The graphs depict policy rules for the level impact as functions of the two state variables. On the horizontal axis is temperature in the range from 0°C to 5°C. The lines represent various levels of the capital share: dark lines (——) depict $S = 0.95$, gray lines (——) refer to $S = 0.5$, and light (——) lines to $S = 0.05$. a) plots green investment as a fraction of green capital, b) shows dirty investment as a fraction of dirty capital, c) depicts consumption as a fraction of output, d) shows green energy as a fraction of green capital, e) depicts fossil fuel use as a fraction of dirty capital, and f) shows the optimal carbon tax as a fraction of total capital.

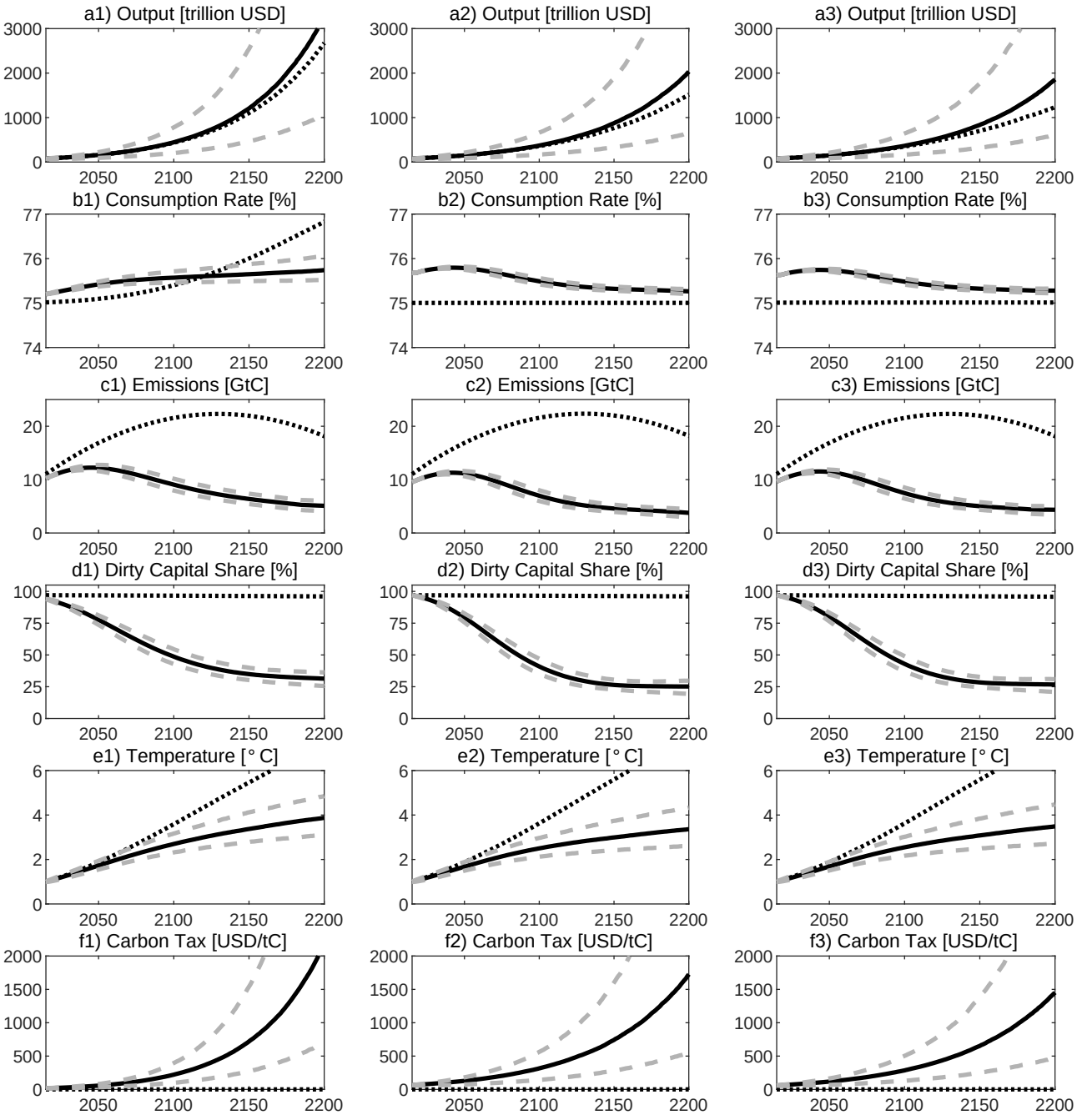


**Figure 6: Evolution of Temperature, the Social Cost of Carbon and the Real Economy.** The figure depicts the simulation of the real economy for the three damage specifications level impact (1st column), disaster impact (2nd column) and growth rate impact (3rd column) until the year 2200. Optimal paths are depicted by solid lines (——) and BAU paths by dotted lines (·····). Dashed lines (- - -) show 5% and 95% quantiles of the optimal solution. Panels a1)-a3) show the evolution of output. Panels b1)-b3) depict the consumption rate expressed as a fraction of output, i.e., $C/Y$. Panels c1)-c3) depict the evolution of carbon emissions. Panels d1)-d3) show the evolution of the share of dirty capital $S$. Panels e1)-e3) depict the evolution of global average temperature increase and Panels f1)-f3) show the optimal carbon tax.

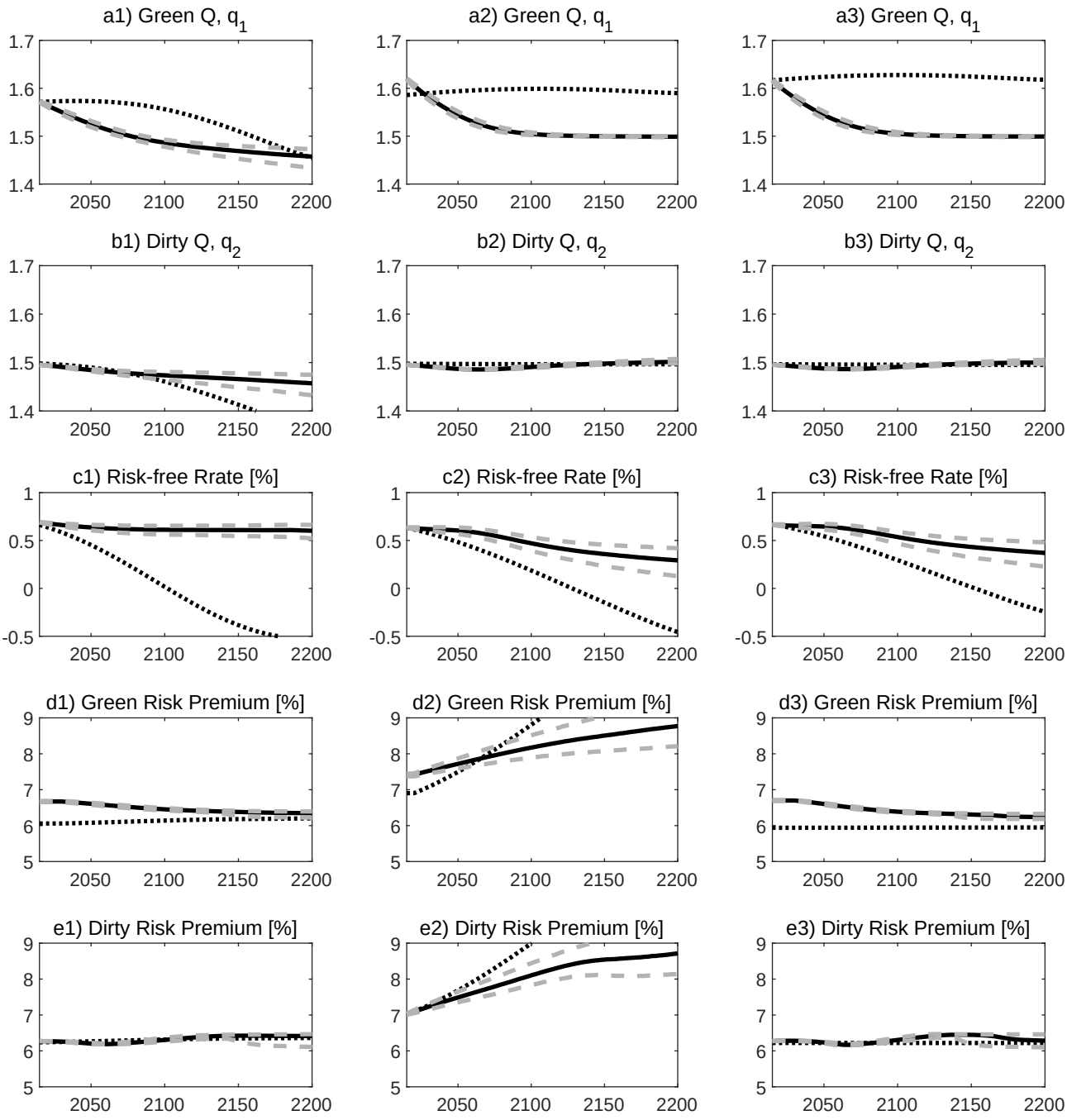


**Figure 7: Evolution of Tobin's Q's, Risk-Free Rates and the Risk Premiums.** The figure depicts the simulation of the asset pricing quantities for the three damage specifications level impact (1st column), disaster impact (2nd column) and growth rate impact (3rd column) until the year 2200. Optimal paths are depicted by solid lines (——) and BAU paths by dotted lines (·····). Dashed lines (- - -) show 5% and 95% quantiles of the optimal solution. Panels a1)-a3) show the evolution of the Tobin's Q of the green asset and Panels b1)-b3) depict the evolution of the Tobin's Q of the dirty asset. Panels c1)-c3) depict the evolution of the equilibrium risk-free rate. Panels d1)-d3) show the evolution of the risk premium of the green asset. Panels e1)-e3) depict the evolution of the risk premium of the dirty asset.